Ultrahigh energy neutrinos and low x physics

Anna Staśto

PennState
Eberly College of Science

ECT, Saturation and Diffraction at the LHC and the EIC, July 1, 2021*

Outline

- Neutrino cross sections at high energy
- Cross section for charm production: comparison with hadronic data
- Nuclear effects
- Forward charm production
- Prompt neutrino fluxes
- Neutrinos from magnetars

A. Bhattacharya, R. Enberg, M. H. Reno, I. Sarcevic, AS
A. Bhattacharya, R. Enberg, Y. S. Jeong, C. S. Kim, M. H. Reno, I. Sarcevic, AS
J. Alonso-Carpio, K. Murase, M. H. Reno, I. Sarcevic, AS

Neutrino astronomy

- Universe not transparent to extragalactic photons with energy > 10 TeV
- Weakly interacting: neutrinos can travel large distances without distortion

Interaction lengths (at 1 TeV):

$$\mathcal{L}_{\rm int}^{\gamma} \sim 100\,{\rm g/cm^2}$$

$$\mathcal{L}_{\rm int}^{\nu} \sim 250 \times 10^9\,{\rm g/cm^2}$$

- Trajectories of protons and nuclei are distorted by the magnetic fields
- Neutrinos can point back to their sources

Angular distortion

$$\delta\phi \simeq \frac{0.7^o}{(E_\nu/{\rm TeV})^{0.7}}$$

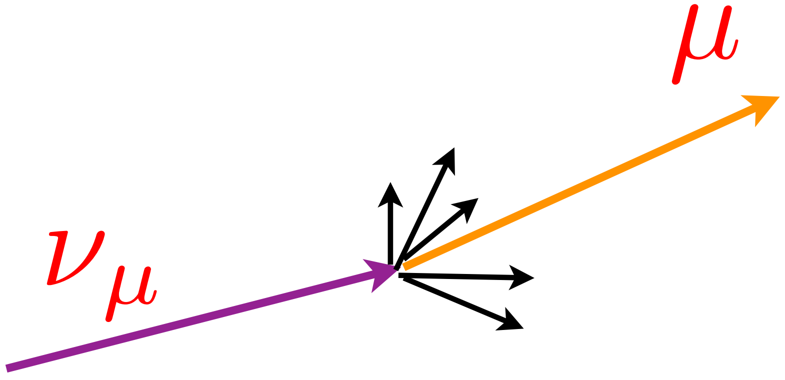

Sources of high energy neutrinos

- Atmospheric: interactions of cosmic rays with nuclei in the atmosphere.
- Interactions of cosmic rays with gas, for example around supernova remnants. Interaction with microwave background (GZK neutrinos).
- Production at some source: radio galaxies, Active Galactic Nuclei, Gamma Ray bursts. Magnetars.
- More exotic scenarios: WIMP annihilation (in the center of Sun or Earth), decays of metastable relic particles,...

IceCube

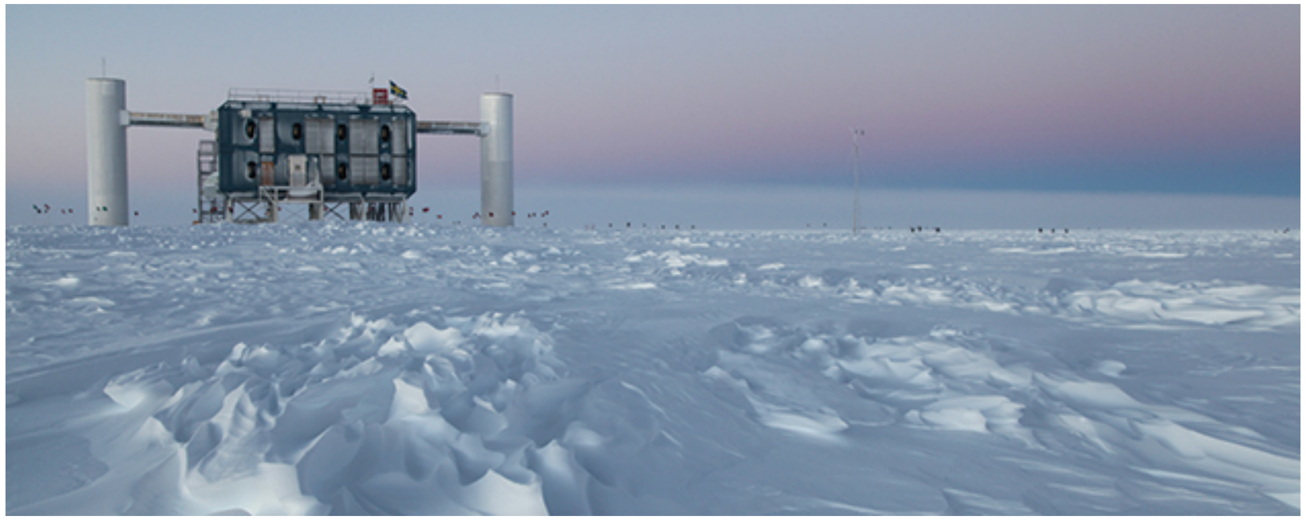

- UHE neutrinos measured in IceCube Antarctic detector
- Neutrinos detected using Cherenkov light produced by charged particles after neutrinos interact
- Sensitivity to high energy >100 GeV neutrinos (>10 GeV with Deep Core)

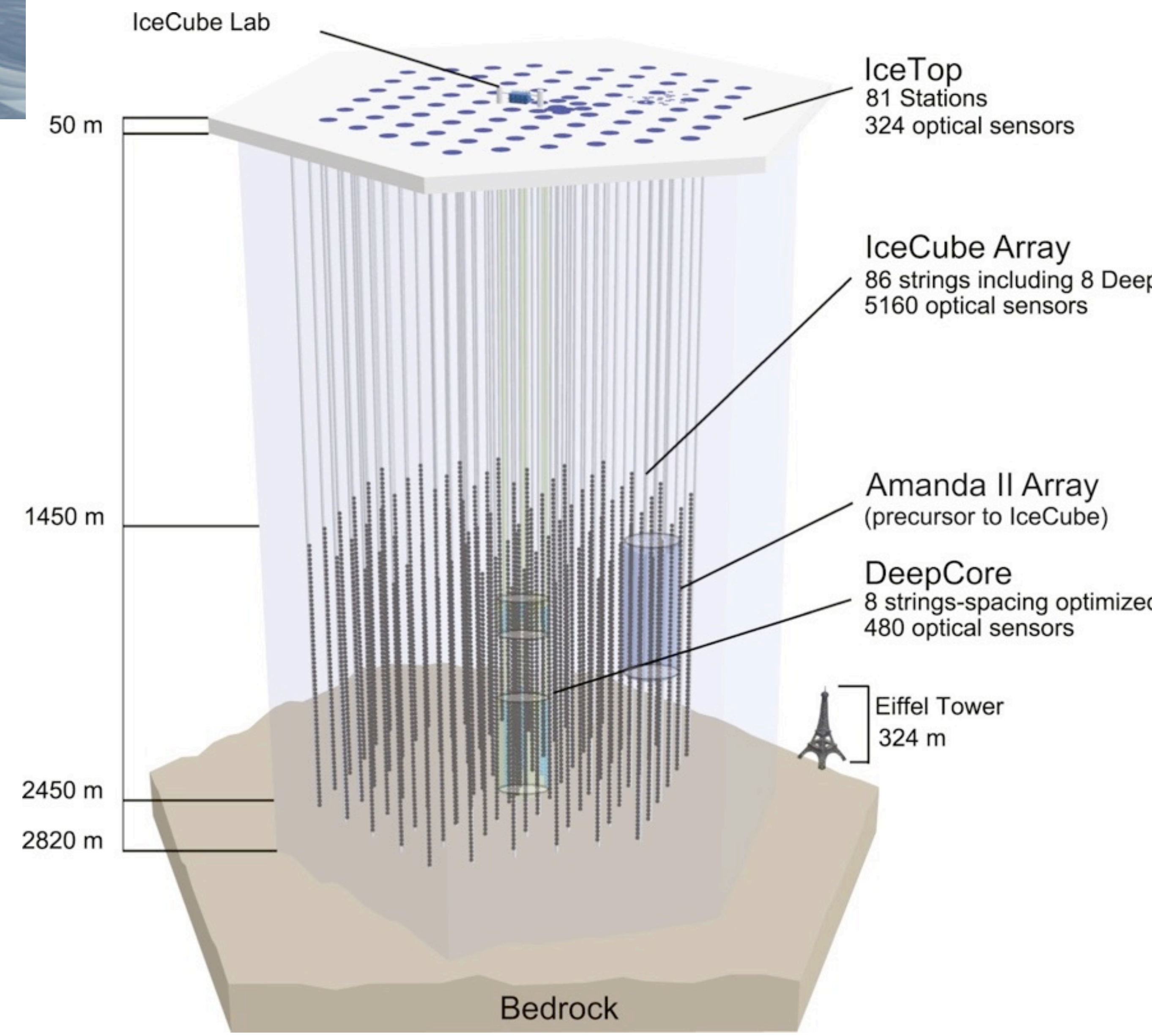

IceCube results

Two classes of events:

Showers: from secondary charged leptons and hadron dissociation

Tracks: events accompanied by an energetic muon (CC events with incoming ν_μ)

Evidence for High-Energy Extraterrestrial Neutrinos at the IceCube Detector

IceCube Collaboration*

SCIENCE VOL 342 22 NOVEMBER 2013

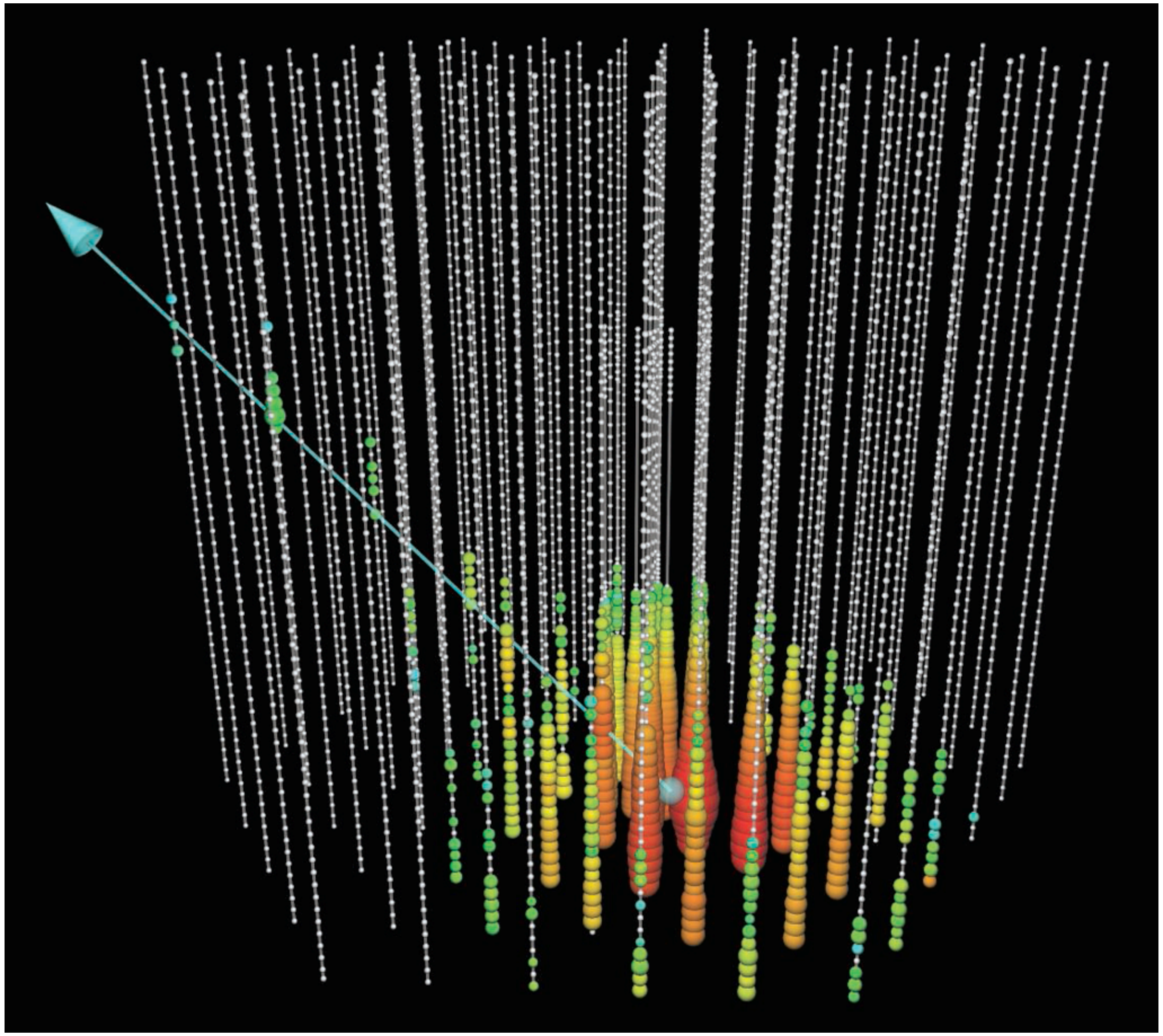

A 250 TeV neutrino interaction in IceCube. At the neutrino interaction point (bottom), a large particle shower is visible, with a muon produced in the interaction leaving up and to the left. The direction of the muon indicates the direction of the original neutrino.

Astrophysical vs atmospheric neutrinos

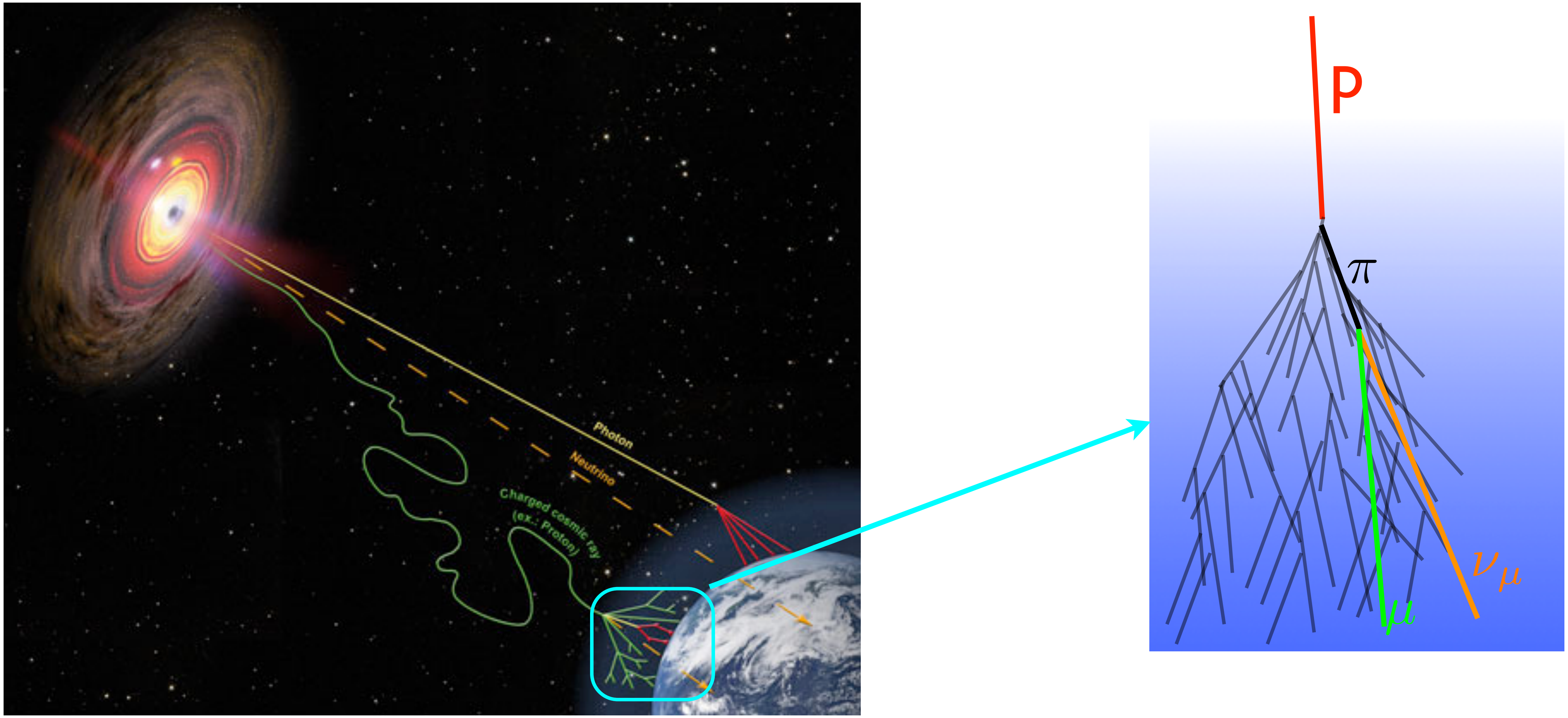

(credit: www.hap-astroparticle.org/ A. Chantelauze)

$p + \mathrm{Air}$

interaction ↓

π, K

decay ↓

μ, ν_μ

Neutrinos in the atmosphere originate from the interactions of cosmic rays (etc. protons) with nuclei.

Neutrino cross sections

Contribution to the cross section in Q and x plane.

$$\frac{d^2\sigma^{CC}}{dxdy} = \frac{2G_F^2 M_N E_\nu}{\pi}\left(\frac{M_W^2}{Q^2+M_W^2}\right)^2 \cdot \left[xq(x,Q^2) + x\bar{q}(x,Q^2)(1-y)^2\right]$$

$$xQ^2\frac{d^2\sigma}{dxdQ^2}$$

$xq(x,Q^2), x\bar{q}(x,($

Since $xq(x,Q^2)$

Need e

vic

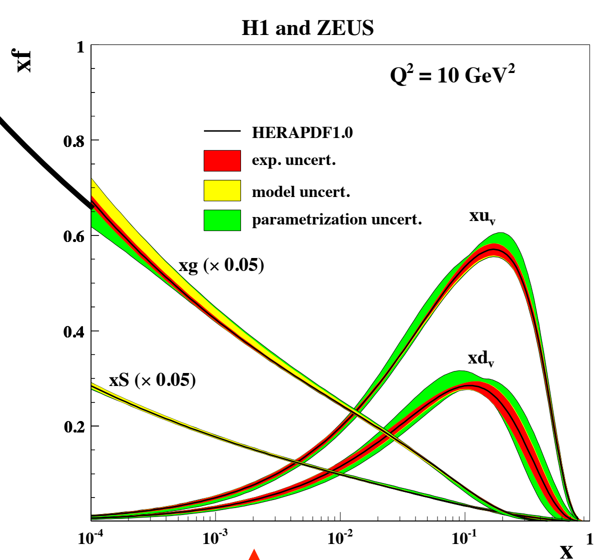

$E_\nu = 10^6$ GeV

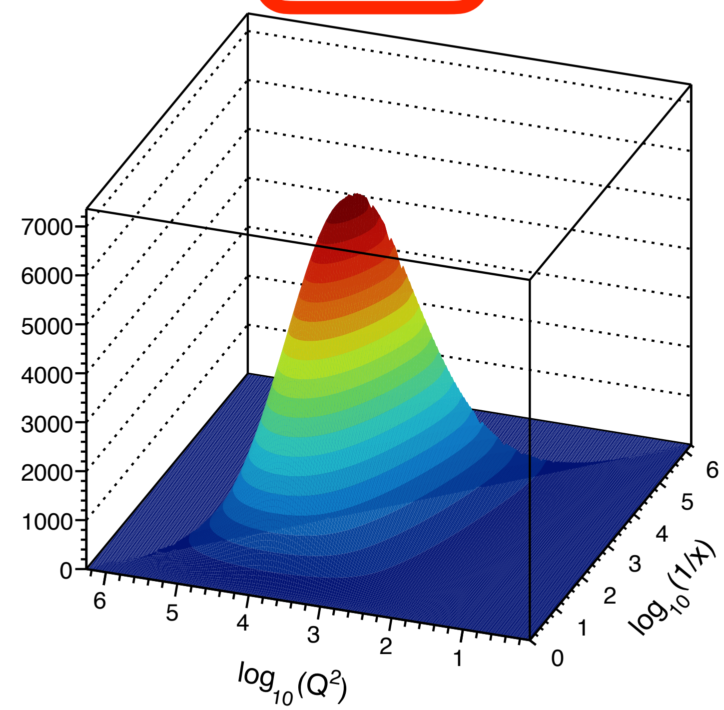

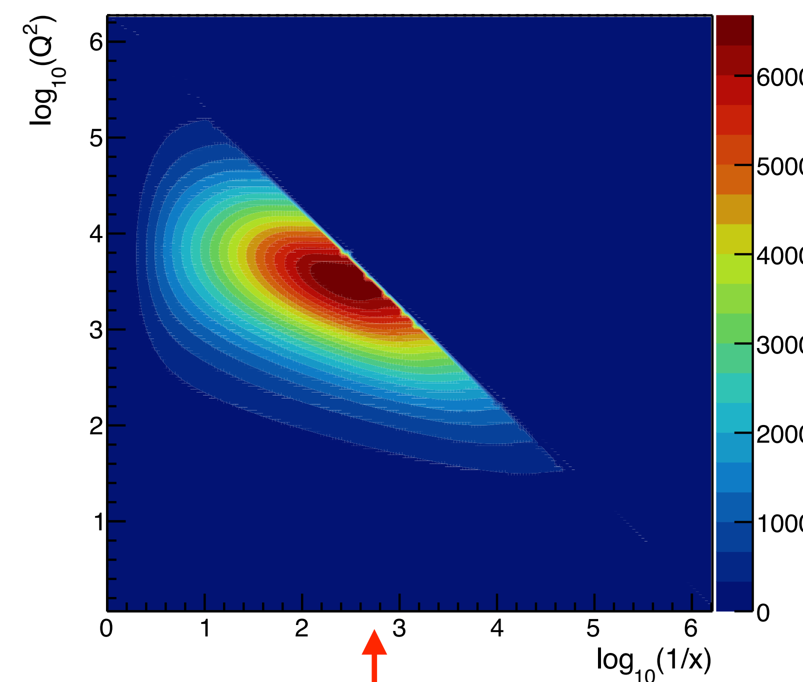

$E_\nu = 10^{11}$ GeV

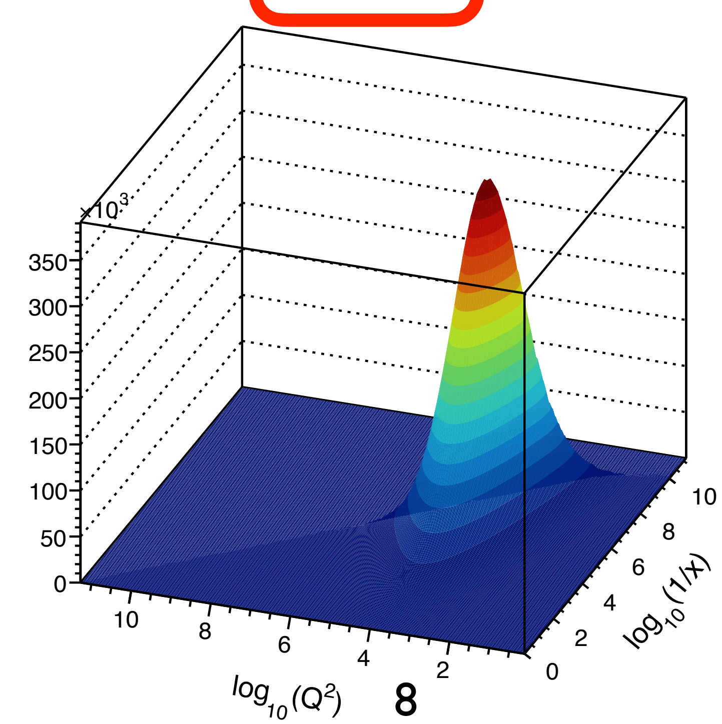

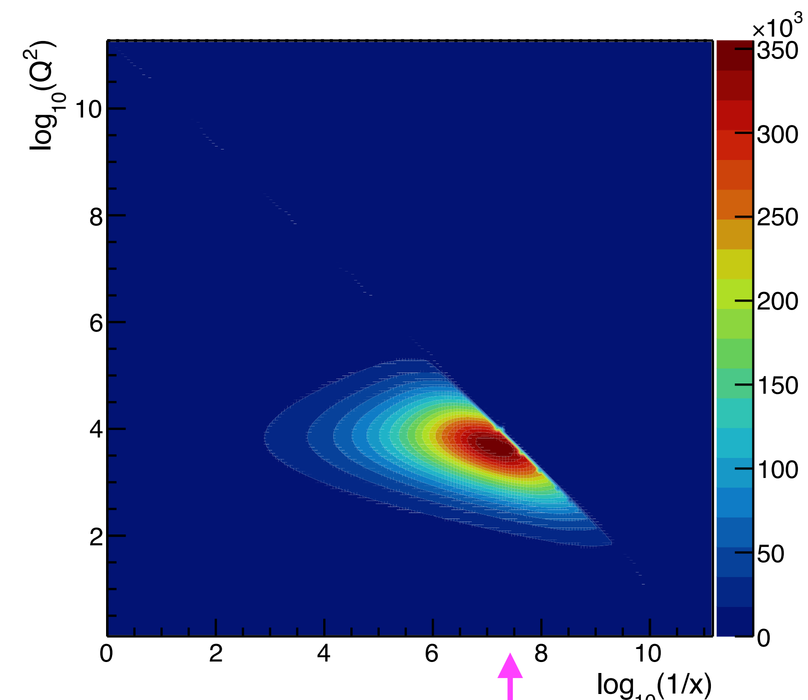

Neutrino cross sections

Kwiecinski,Martin,AS

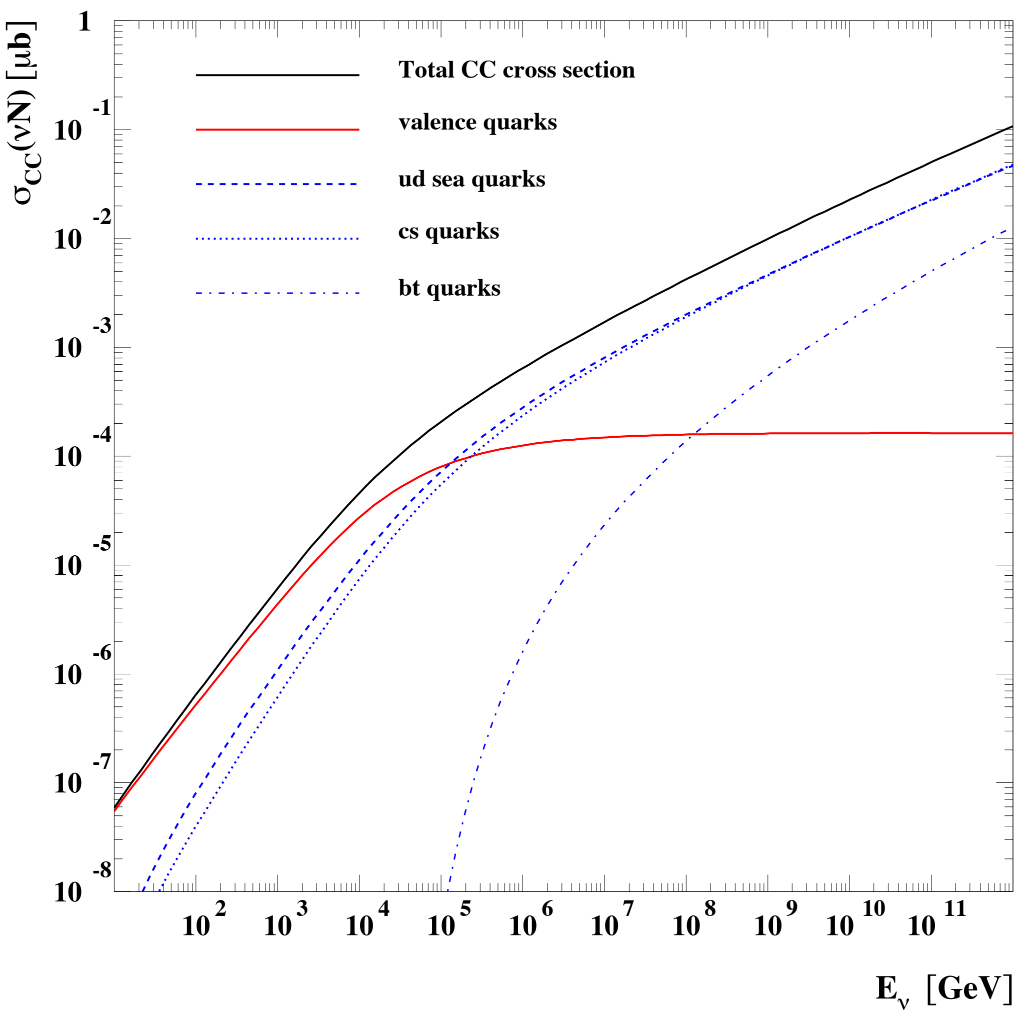

Calculation of the neutrino cross section using unified DGLAP/BFKL evolution: including small x resummation effects.

ICECUBE result

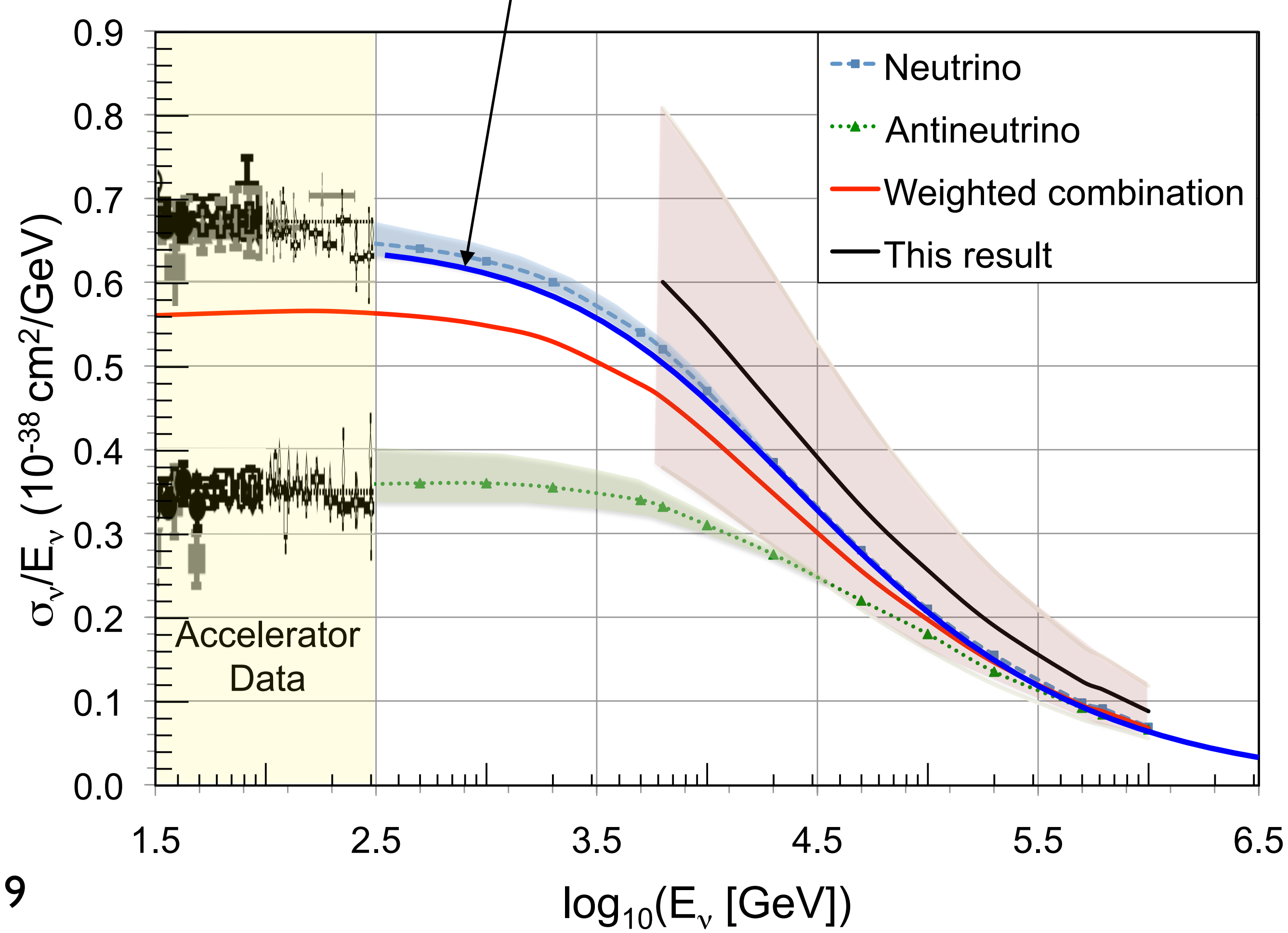

Resummation predictions are very stable: consistent with the more recent standard DGLAP extrapolations and the new measurement by the ICECUBE collaboration (the sampled x values are not very small for this kinematics though)

Neutrino cross sections

Nuclear ratio (relative to deuterium) of cross sections for neutrinos and antineutrinos as a function of (anti)neutrino energy EPPS16

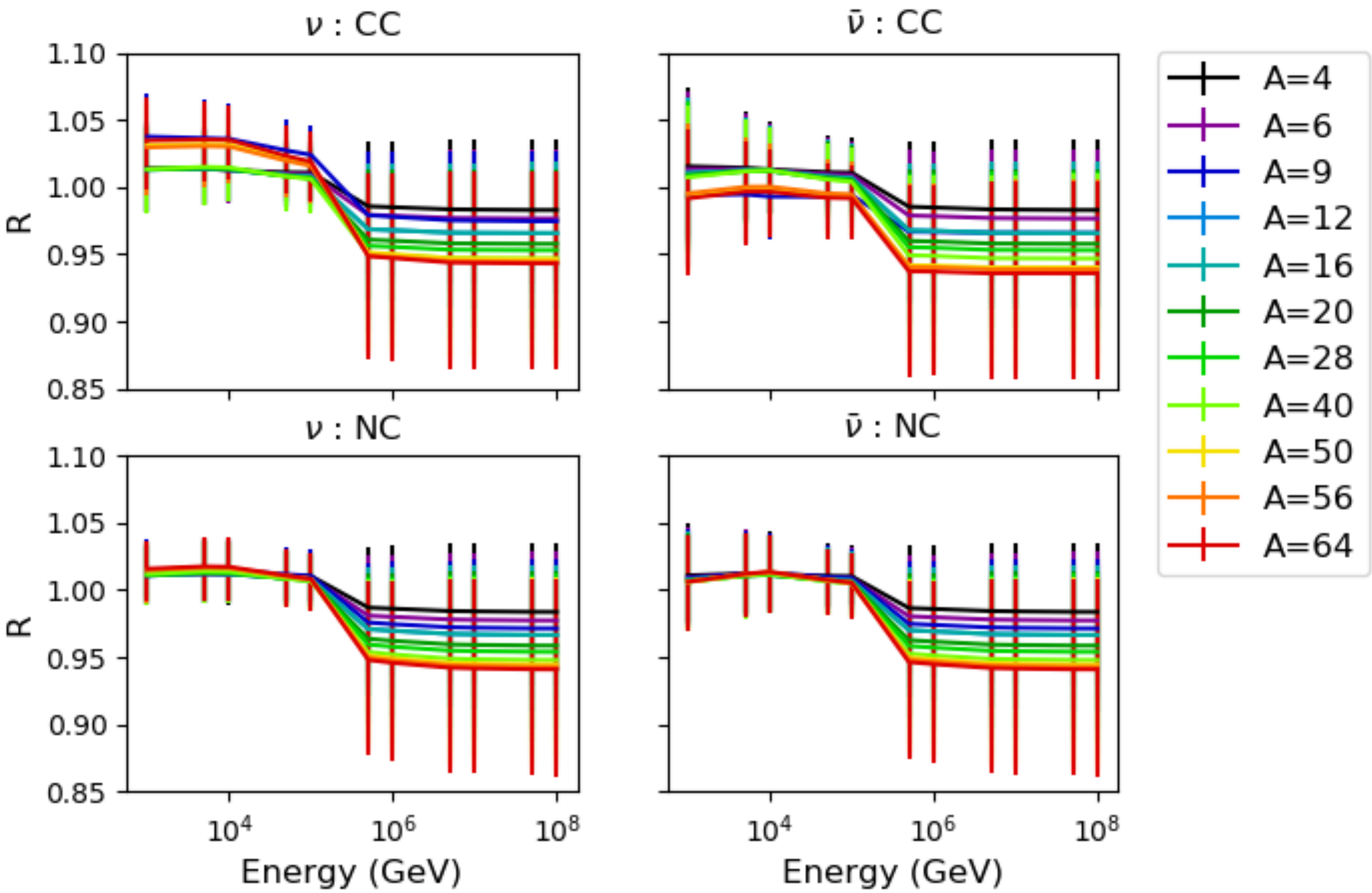

Klein, Robertson, Vogt

Nuclear ratio of interaction probabiity as a function of energy and zenith angle. Shadowing (R<1) and antishadowing (R>1) visible.

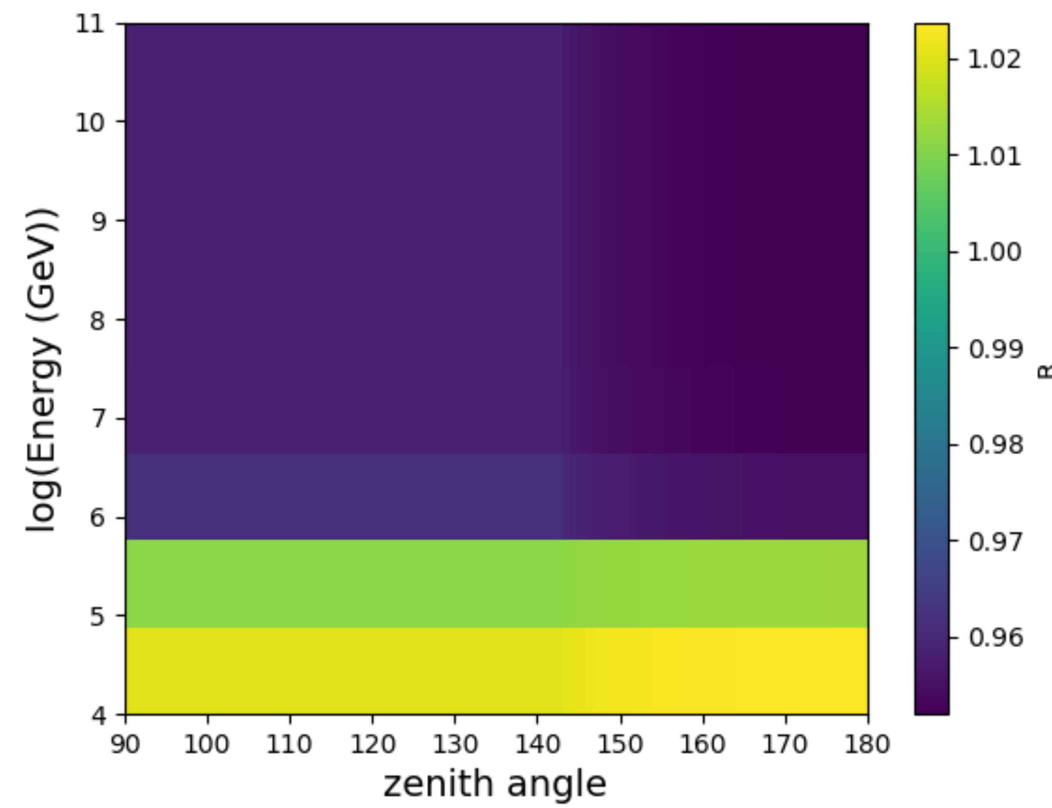

Nuclear effects expected to be small. CGC effects not taken into account, could have bigger impact.

Atmospheric neutrinos

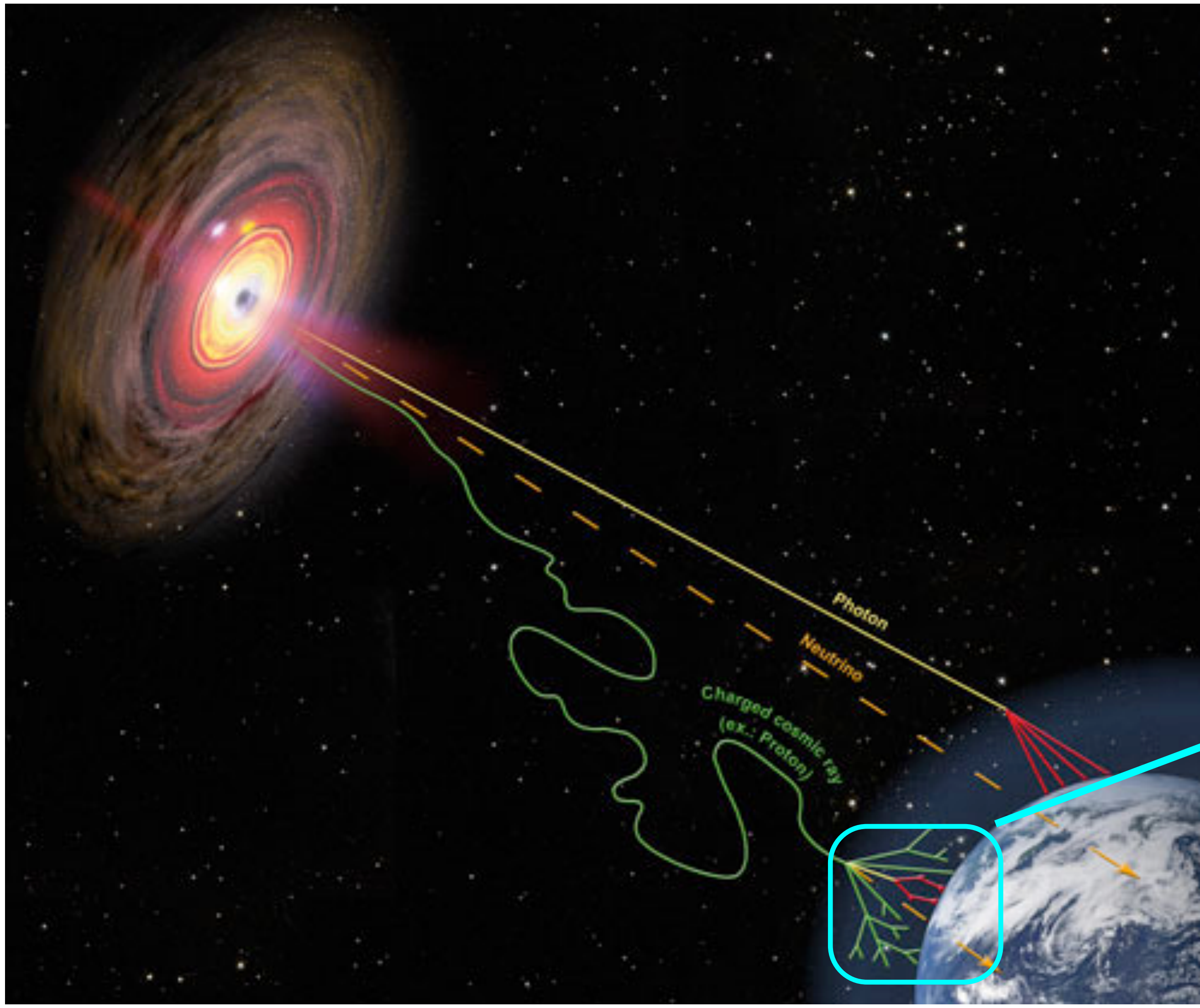

(credit: www.hap-astroparticle.org/ A. Chantelauze)

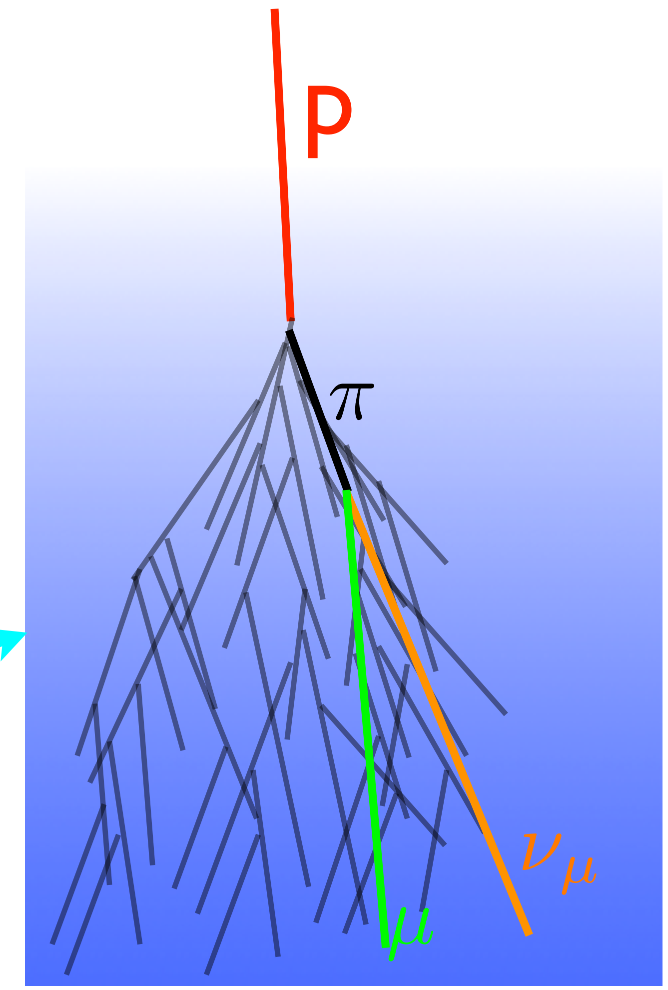

$$p + \text{Air} \xrightarrow{\textit{interaction}} \pi, K \xrightarrow{\textit{decay}} \mu, \nu_\mu$$

Neutrinos in the atmosphere originate from the interactions of cosmic rays (etc. protons) with nuclei.

Neutrinos from meson decays

- *Conventional*: decays of lighter mesons

$\pi^{\pm}, K^{\pm}$

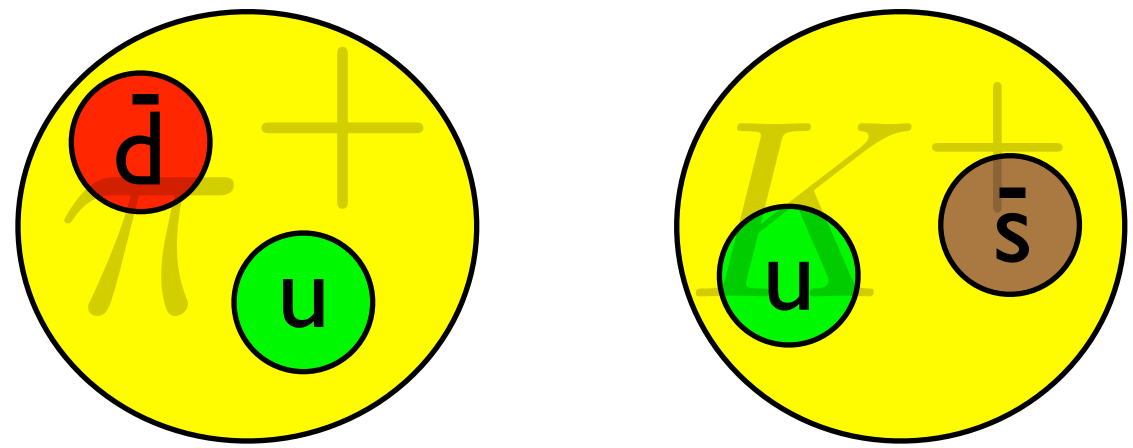

Mean lifetime: $\tau \sim 10^{-8}\ s$

Long lifetime: interaction occurs before decay

$$\mathcal{L}_{\rm int} < \mathcal{L}_{\rm dec}$$

Long-lived mesons loose energy → Steeply falling flux of neutrinos

$$\Phi_\nu \sim E_\nu^{-3.7}$$

Prompt neutrinos

- *Prompt*: decays of heavier, charmed or bottom mesons

$D^{\pm}, D^0, D_s$

baryon Λ_c

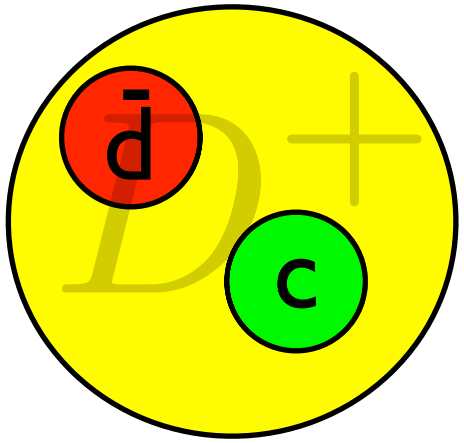

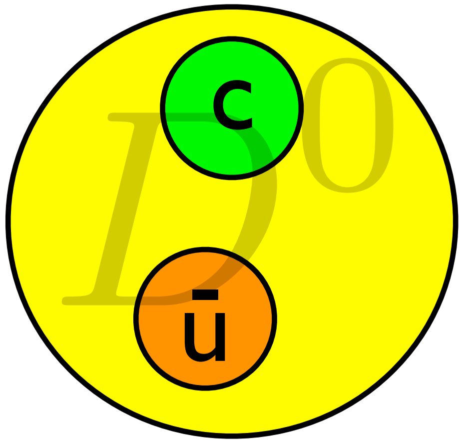

Mean lifetime: $\tau \sim 10^{-12}\ s$

Short lifetime: decay, no interaction

$$\mathcal{L}_{\rm int} > \mathcal{L}_{\rm dec}$$

Flat flux, more energy transferred to neutrino

$$\Phi_\nu \sim E_\nu^{-2.7}$$

Prompt vs conventional flux

High energy atmospheric neutrino flux as a function of energy

conventional: decay of long lived pions and kaons: loose energy.
Soft spectrum.

prompt: decay of short lived charmed mesons: do not loose energy.
Hard spectrum.

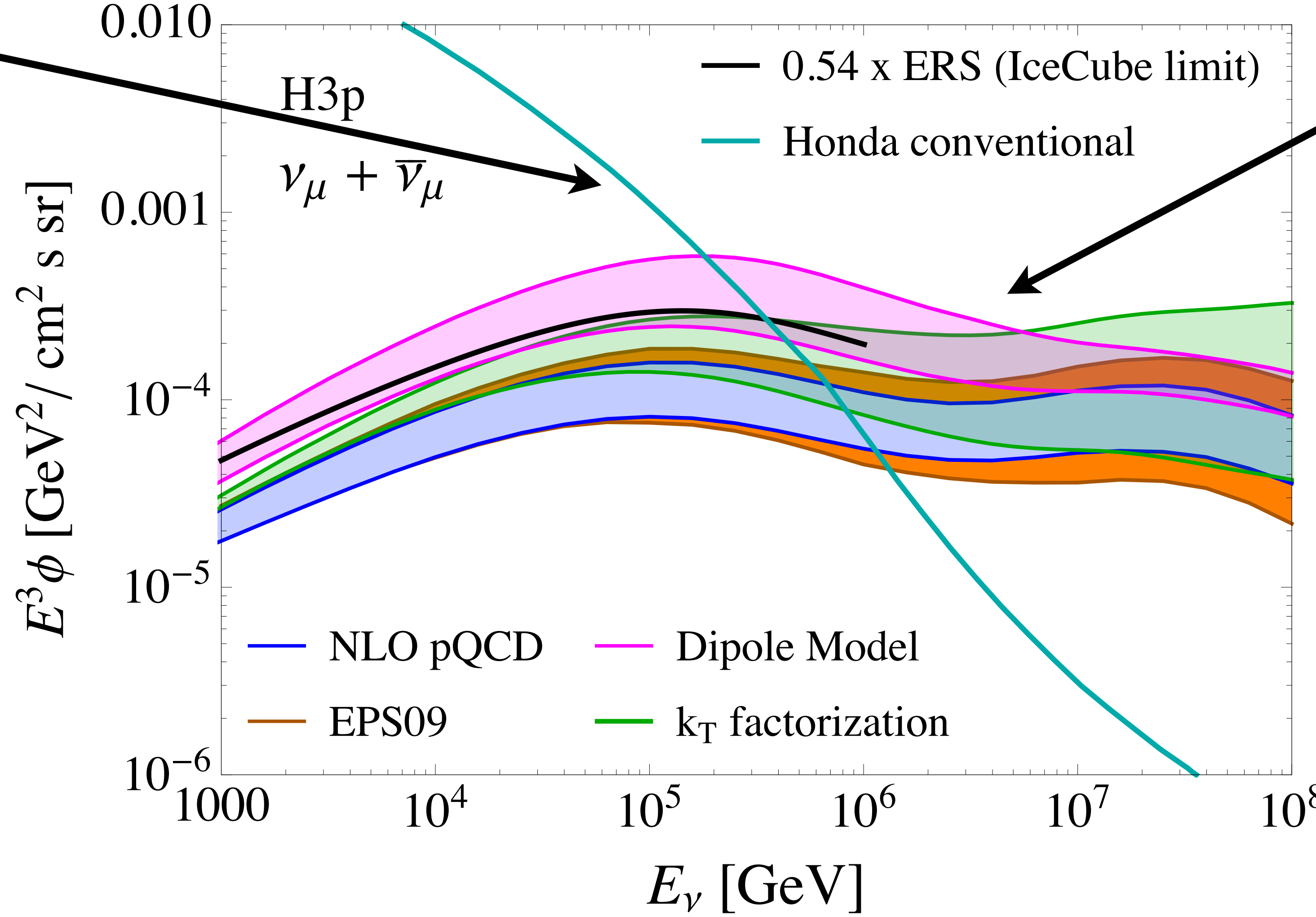

- Conventional flux: constrained by the low energy neutrino data.

- Prompt flux: poorly known, large uncertainties. Essential to evaluate as it can dominate the background for searches for extraterrestrial high energy neutrinos.

From cosmic ray to neutrino detection

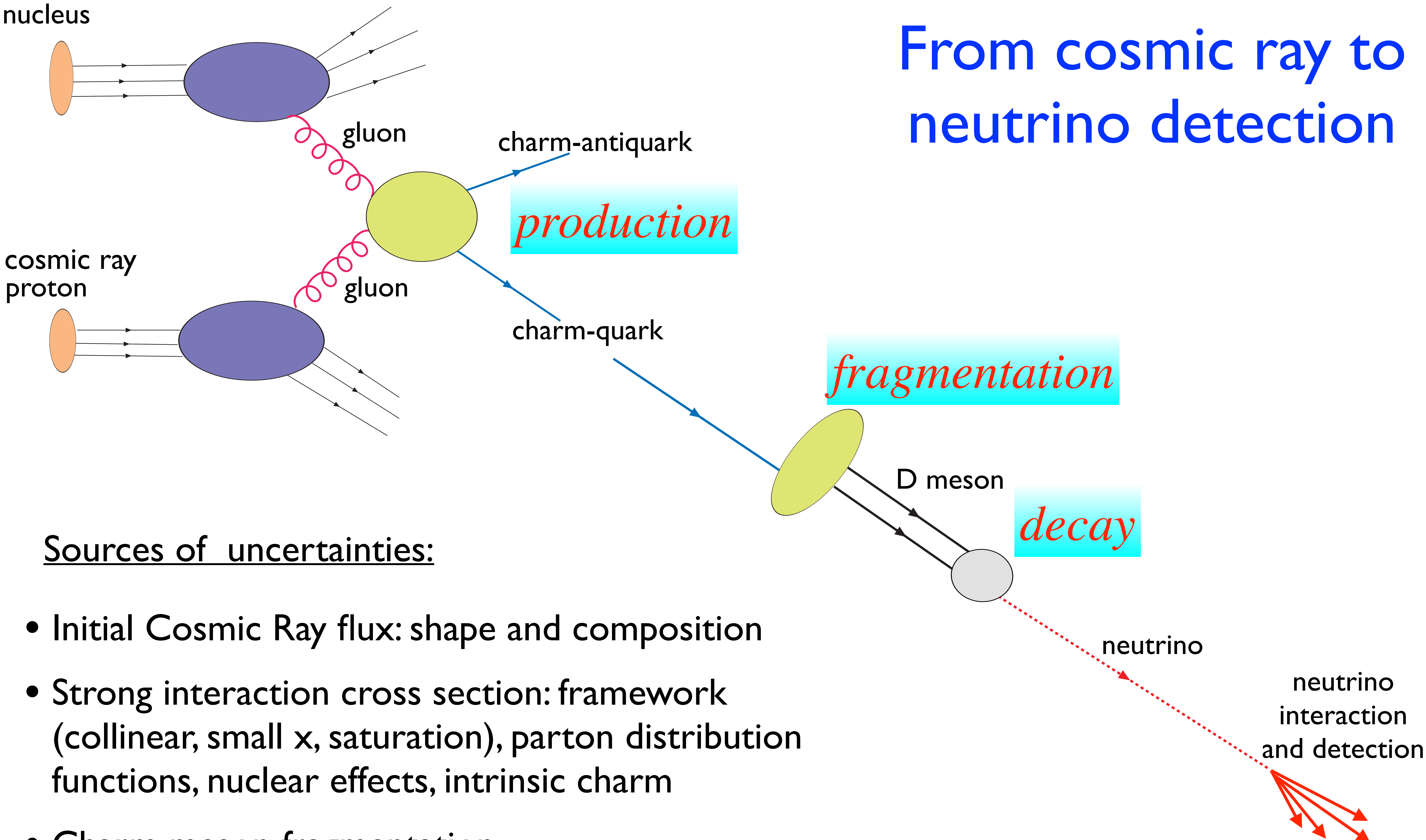

Sources of uncertainties:

- Initial Cosmic Ray flux: shape and composition
- Strong interaction cross section: framework (collinear, small x, saturation), parton distribution functions, nuclear effects, intrinsic charm
- Charm meson fragmentation
- Decay
- Interaction cross section of neutrino

Frameworks for heavy quark production

- Standard NLO perturbative QCD collinear calculation.
- High-energy factorization with small x BFKL/DGLAP resummed evolution, including saturation effects (through nonlinear evolution equation).
- Small x dipole model with saturation.

Also:

Nuclear corrections.

b quark contribution.

Heavy quark production in hadron collisions

Schematic representation of charm production in pp scattering:

$f_i(x,\mu)$ parton distribution function at scale μ
parametrized at scale μ_0
evolved to higher scales with QCD evolution equations

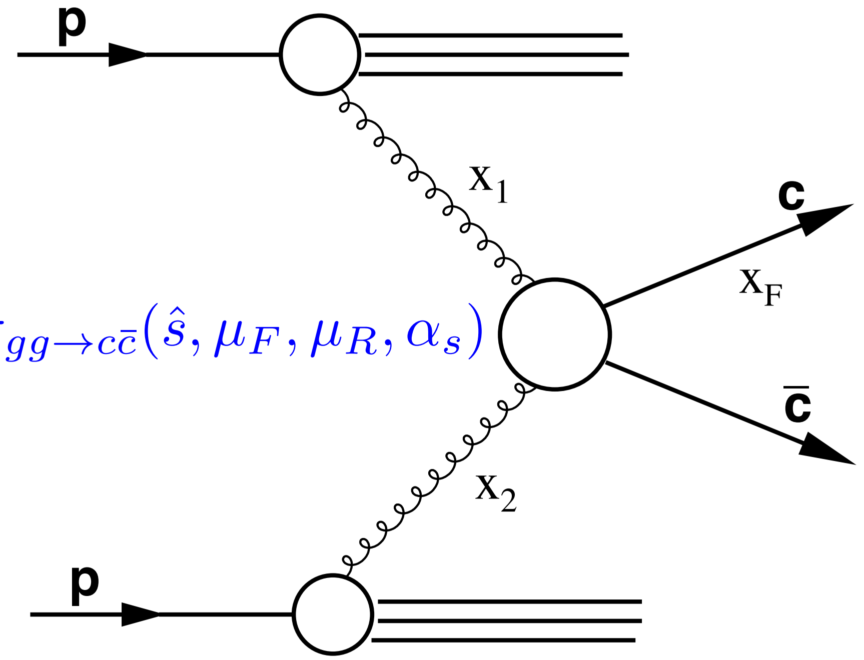

x_1, x_2 longitudinal momentum fractions (of a proton momentum) of gluons participating in a scattering process

$\hat{\sigma}_{gg\to c\bar{c}}(\hat{s},\mu_F,\mu_R,\alpha_s)$ partonic cross section calculable in a perturbative way in QCD

Factorization formula for cross section:

$$\frac{d\sigma^{pp\to c+X}}{dx_F} = \sum_{i,j} f_i(x_1,\mu_F)\otimes\hat{\sigma}_{gg\to c\bar{c}}(\hat{s},m_c,\mu_F,\mu_R)\otimes f_j(x_2,\mu_F)$$

Low x parton density

$$\frac{d\sigma^{pp\to c+X}}{dx_F} = \sum_{i,j} f_i(x_1,\mu_F) \otimes \hat{\sigma}_{gg\to c\bar{c}}(\hat{s}, m_c, \mu_F, \mu_R) \otimes f_j(x_2,\mu_F)$$

For the cosmic ray interactions we are interested in the forward production: charm quark is produced with very high fraction of the momentum of the incoming cosmic ray projectile. Other participating gluon will have very small fraction of longitudinal momentum:

$$x_F \simeq \frac{E_c}{E_p} \qquad x_F \gg x_2 \qquad x_2 \sim \frac{M^2_{c\bar{c}}}{x_F s}$$

$$s \gg M^2_{c\bar{c}}$$

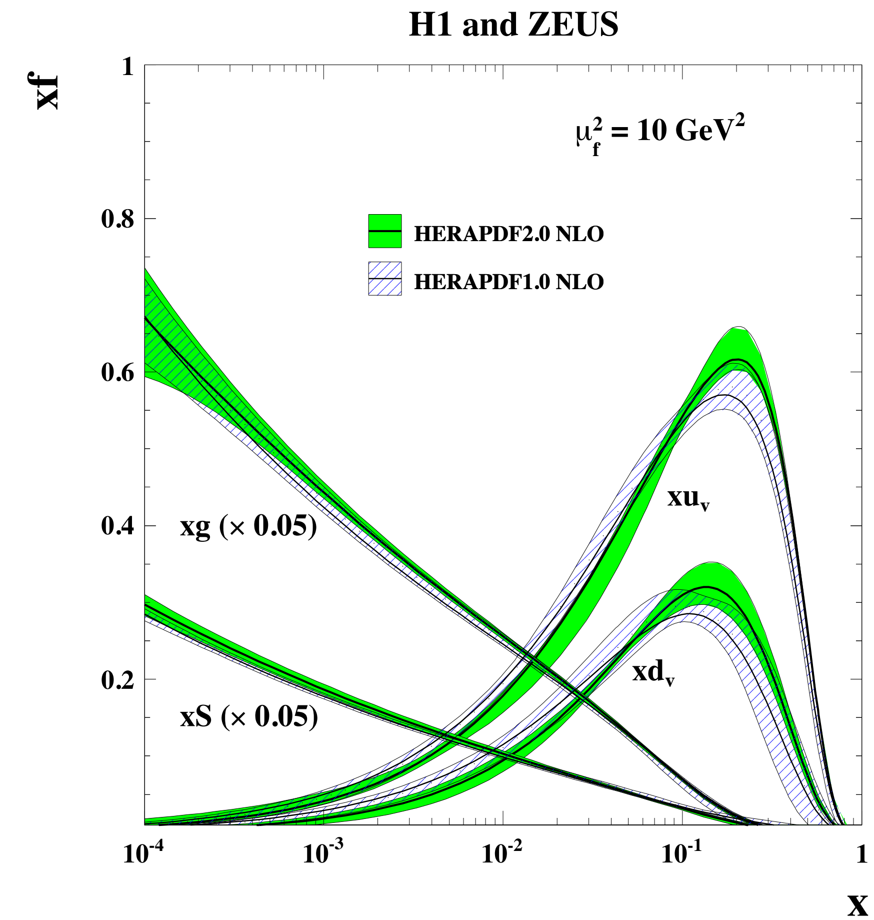

The cross section is sensitive to the domain of parton densities which are at very small values of x. This is poorly constrained region.

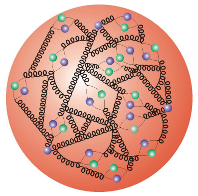

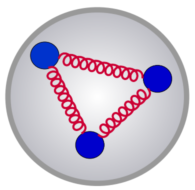

<u>Other approaches tested:</u>

Small x resummation + high energy factorization

Dipole model

Hybrid k_T factorization calculation

Use k_T factorization with off-shell gluon and unintegrated parton density.
Suitable for the high energy - low x regime.
Since it is forward production, use hybrid calculation: treat large x gluon as collinear, and small x gluon as off-shell.

collinear gluon

$$\sigma(pp \to q\bar{q}X) = \int \frac{dx_1}{x_1}\frac{dx_2}{x_2}\, dz\, dx_F\, \delta(zx_1 - x_F)\, x_1 g(x_1, M_F) \times \int \frac{dk_T^2}{k_T^2} \hat{\sigma}^{\rm off}(z, \hat{s}, k_T)\, f(x_2, k_T^2)$$

off-shell gluon with k_T dependence

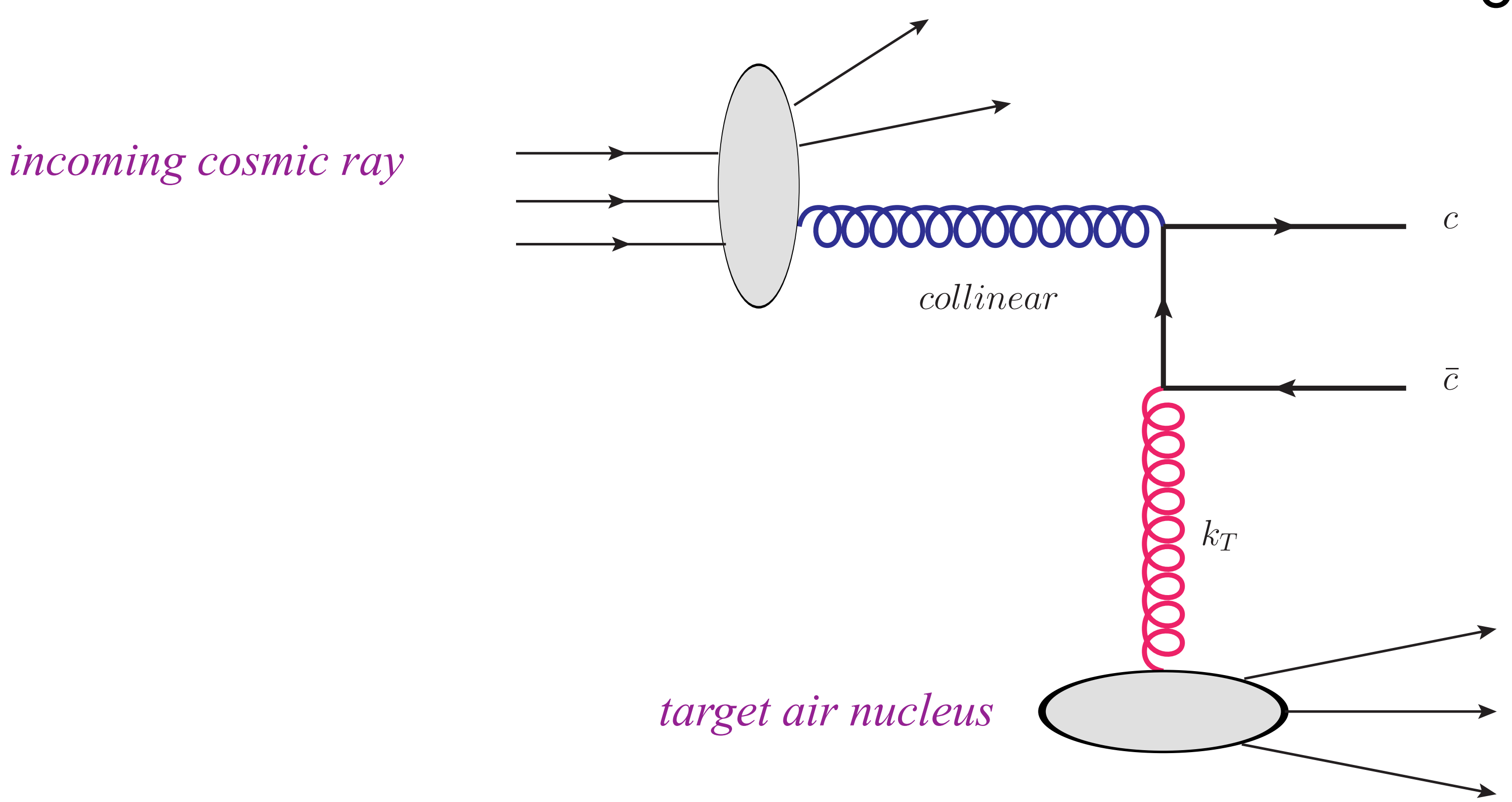

Hybrid k_T factorization calculation

Kutak-Sapeta model

Unintegrated gluon density obtained from the resummed small x evolution equation with non-linear term:

BFKL term with kinematical constraint

$$f(x,k^2) = \tilde{f}^{(0)}(x,k^2) + \\ + \frac{\alpha_s(k^2)N_c}{\pi}k^2\int_x^1\frac{dz}{z}\int_{k_0^2}\frac{dk'^2}{k'^2}\left\{\frac{f(\frac{x}{z},k'^2)\,\Theta(\frac{k^2}{z}-k'^2)\;-\;f(\frac{x}{z},k^2)}{|k'^2-k^2|}+\frac{f(\frac{x}{z},k^2)}{|4k'^4+k^4|^{\frac{1}{2}}}\right\}+ \\ + \frac{\alpha_s(k^2)N_c}{\pi}\int_x^1 dz\,\bar{P}_{gg}(z)\int_{k_0^2}^{k^2}\frac{dk'^2}{k'^2}f(\frac{x}{z},k'^2) - \\ - \left(1-k^2\frac{d}{dk^2}\right)^2\frac{k^2}{R^2}\int_x^1\frac{dz}{z}\left[\int_{k^2}^{\infty}\frac{dk'^2}{k'^4}\alpha_s(k'^2)\ln\left(\frac{k'^2}{k^2}\right)f(z,k'^2)\right]^2$$

DGLAP with non-singular splitting

non-linear term

Nonlinear term responsible for taming the growth of the gluon density

Unintegrated parton density fitted to the inclusive structure function data.

Total charm production cross section

- NLO collinear calculation, HVQ, *Nason, Dawson, Ellis; Mangano, Nason, Ridolfi*
- Default parton distribution set is CT15 Central.
- Charm quark mass $m_c = 1.27 \ \mathrm{GeV}$
- Variation of factorization and renormalization scales with respect to charm quark mass. Using range provided by Nelson, Vogt, Frawley
- Magenta-free nucleons, blue-nitrogen
- Comparison with RHIC and LHC data. Data are extrapolated with NLO QCD from measurements in the limited phase space region.

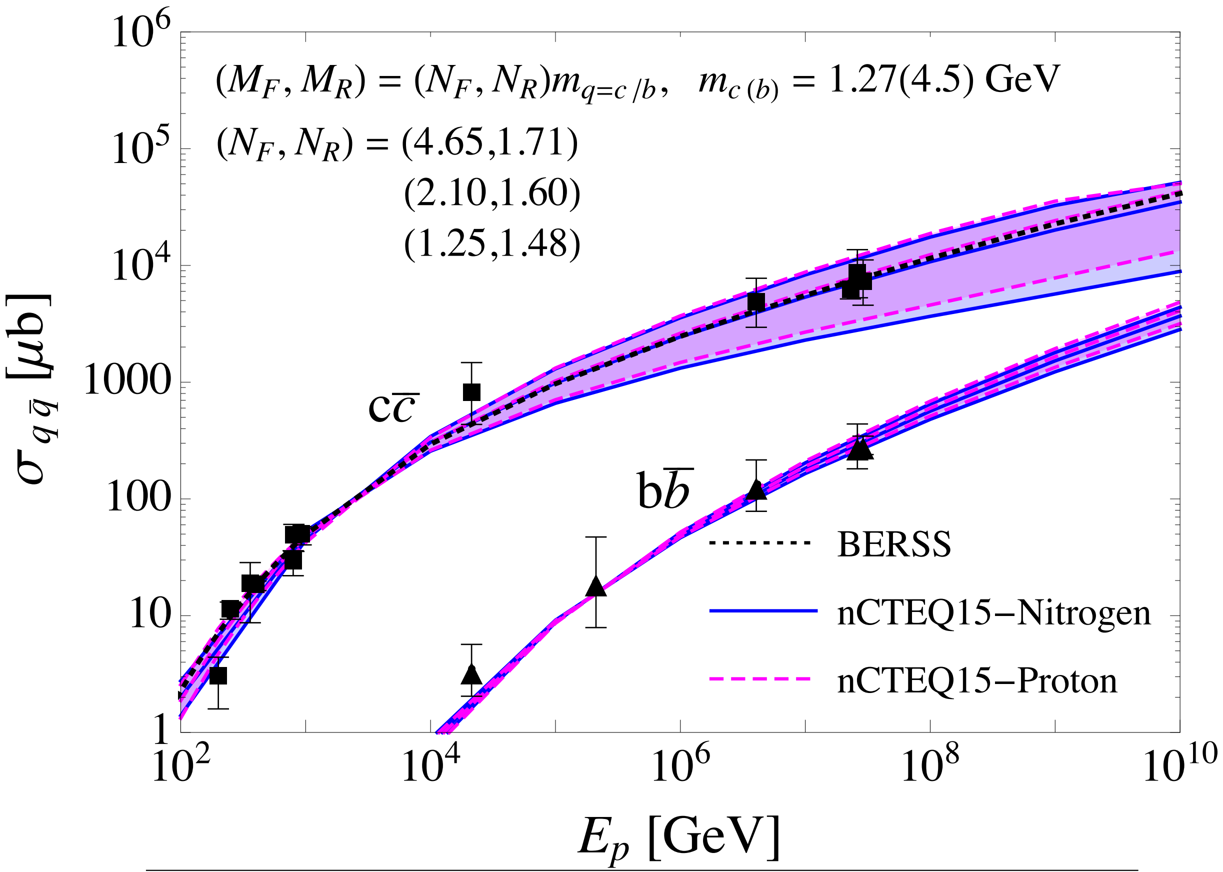

Expt.	$\sqrt{s}$ [TeV]	σ [mb]
PHENIX [31]	0.20	$\mathbf{0.551}^{+0.203}_{-0.231}$ (sys)
STAR [32]	0.20	$\mathbf{0.797} \pm 0.210$ (stat)$^{+0.208}_{-0.295}$ (sys)
ALICE [27]	2.76	$\mathbf{4.8} \pm 0.8$ (stat)$^{+1.0}_{-1.3}$ (sys) ± 0.06 (BR) ± 0.1(frag) ± 0.1 (lum)$^{+2.6}_{-0.4}$ (extrap)
ALICE [27]	7.00	$\mathbf{8.5} \pm 0.5$ (stat)$^{+1.0}_{-2.4}$ (sys) ± 0.1 (BR) ± 0.2(frag) ± 0.3 (lum)$^{+5.0}_{-0.4}$ (extrap)
ATLAS [28]	7.00	$\mathbf{7.13} \pm 0.28$ (stat)$^{+0.90}_{-0.66}$ (sys) ± 0.78 (lum)$^{+3.82}_{-1.90}$ (extrap)
LHCb [30]	7.00	$\mathbf{6.100} \pm 0.930$

Table 1: Total cross-section for $pp(pN) \to c\bar{c}X$ in hadronic collisions, extrapolated based on NLO QCD by the experimental collaborations from charmed hadron production measurements in a limited phase space region.

Total charm production cross section

Comparison with other models: small x resummation-k_T factorization and dipole model

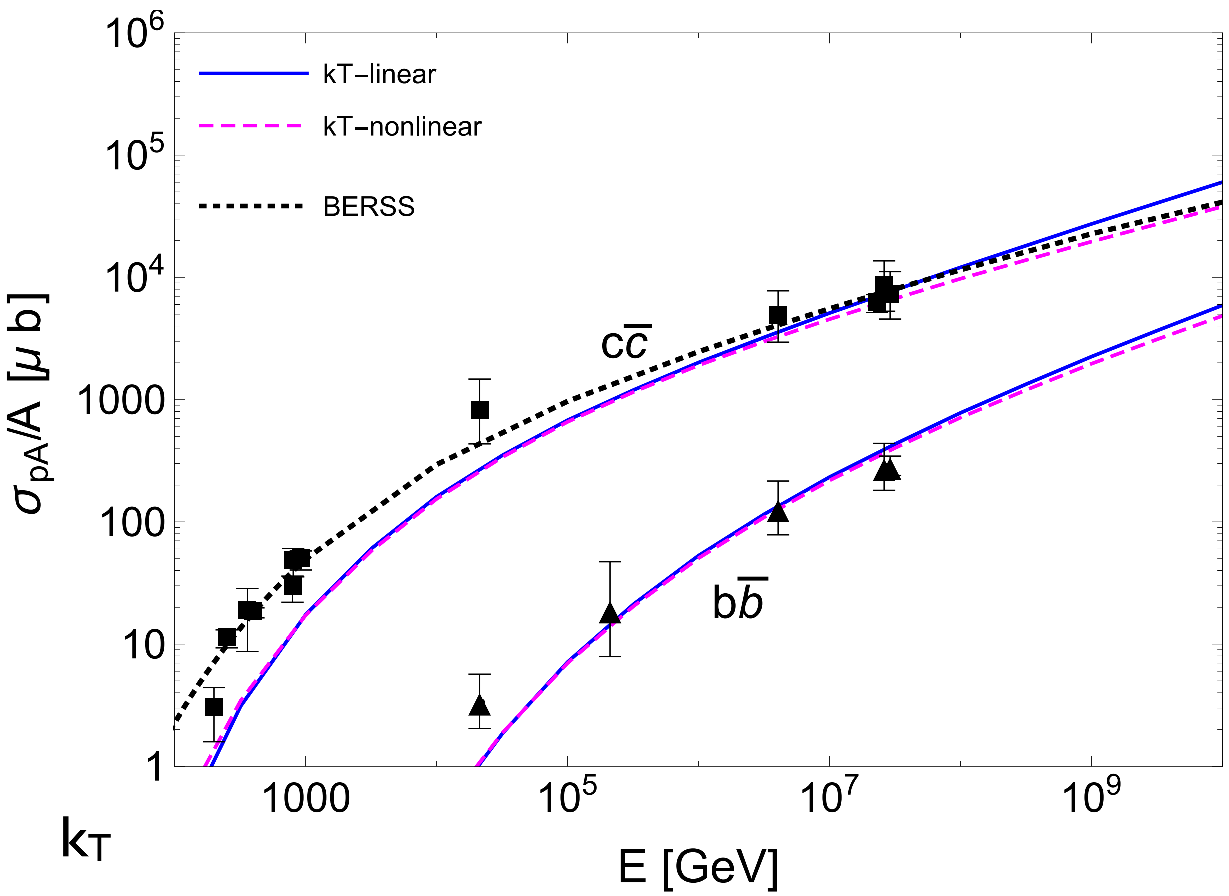

k_T

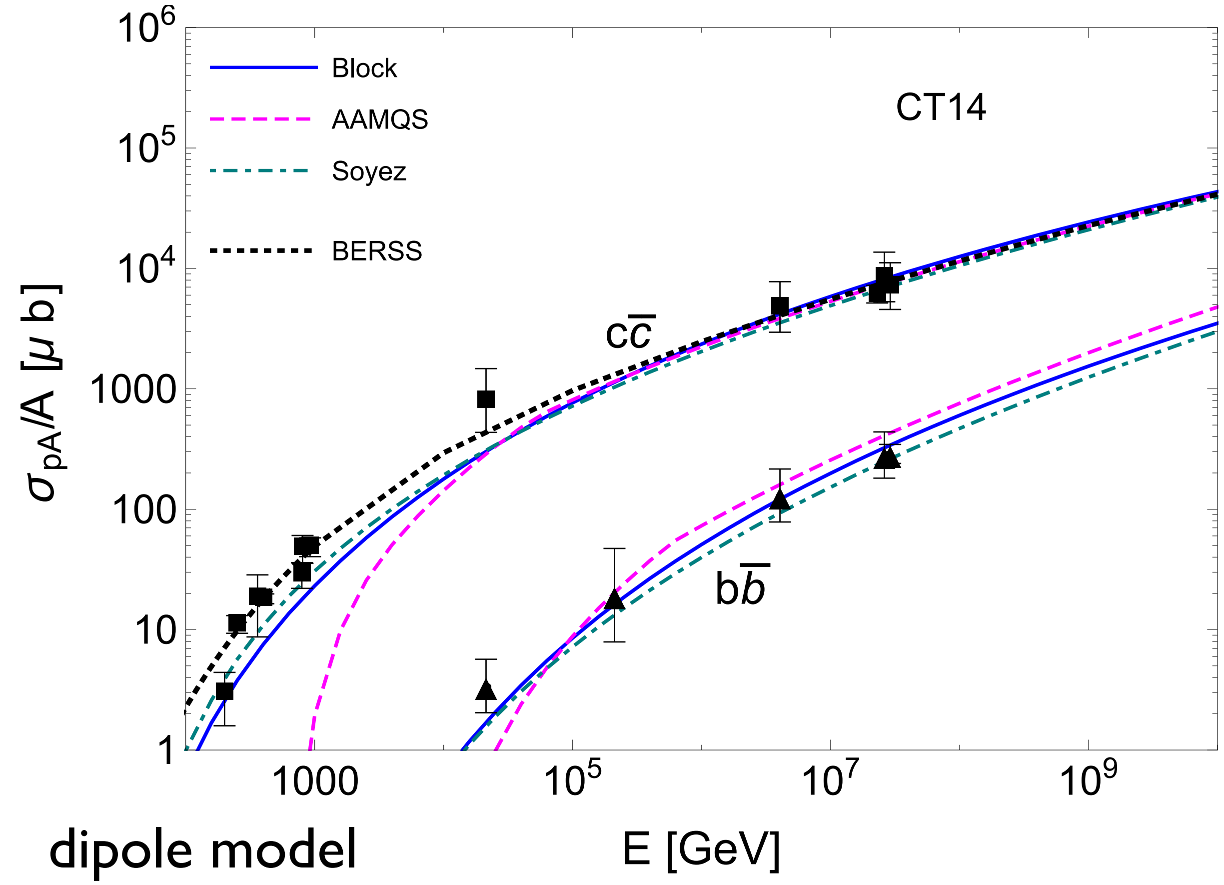

dipole model

- BERSS: *Bhattacharya, Enberg,Reno,Stasto,Sarcevic*: previous NLO calculation
- AAMQS,*Albacete, Armesto,Milhano,Quiroga-Arias,Salgado:* rcBK
- Soyez: based on *Iancu,Itakura,Munier* parametrization inspired by BK solution
- Block: phenomenological parametrization of the structure function
- k_T calculation underestimates data at low energy.
- Need additional diagrams there (or energy dependent K-factor).

All models agree with data at high energies

Nuclear corrections

Need to take into account the fact that the target is not a proton but nitrogen/oxygen. Possible nuclear corrections: shadowing

$$R^A = \frac{\sigma^A}{A\,\sigma^p} \neq 1$$

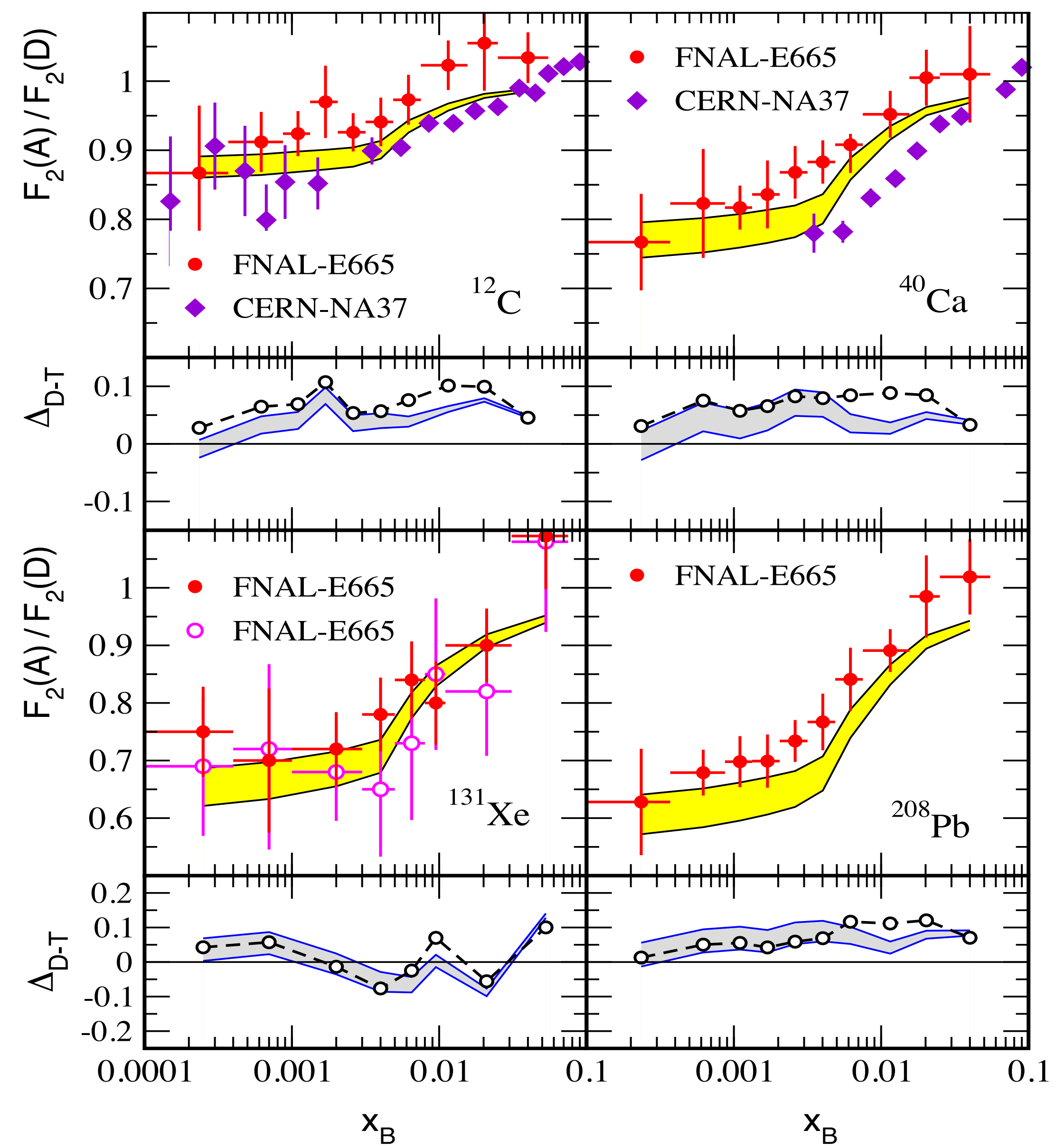

Cross section on nucleus is not a simple superposition of cross sections on nucleons.

Complicated dependence on the kinematical variables as well as mass number.

Nuclear corrections

Nuclear modifications to the total charm production cross section are small:

10%-15% for charm
5%-10% for bottom

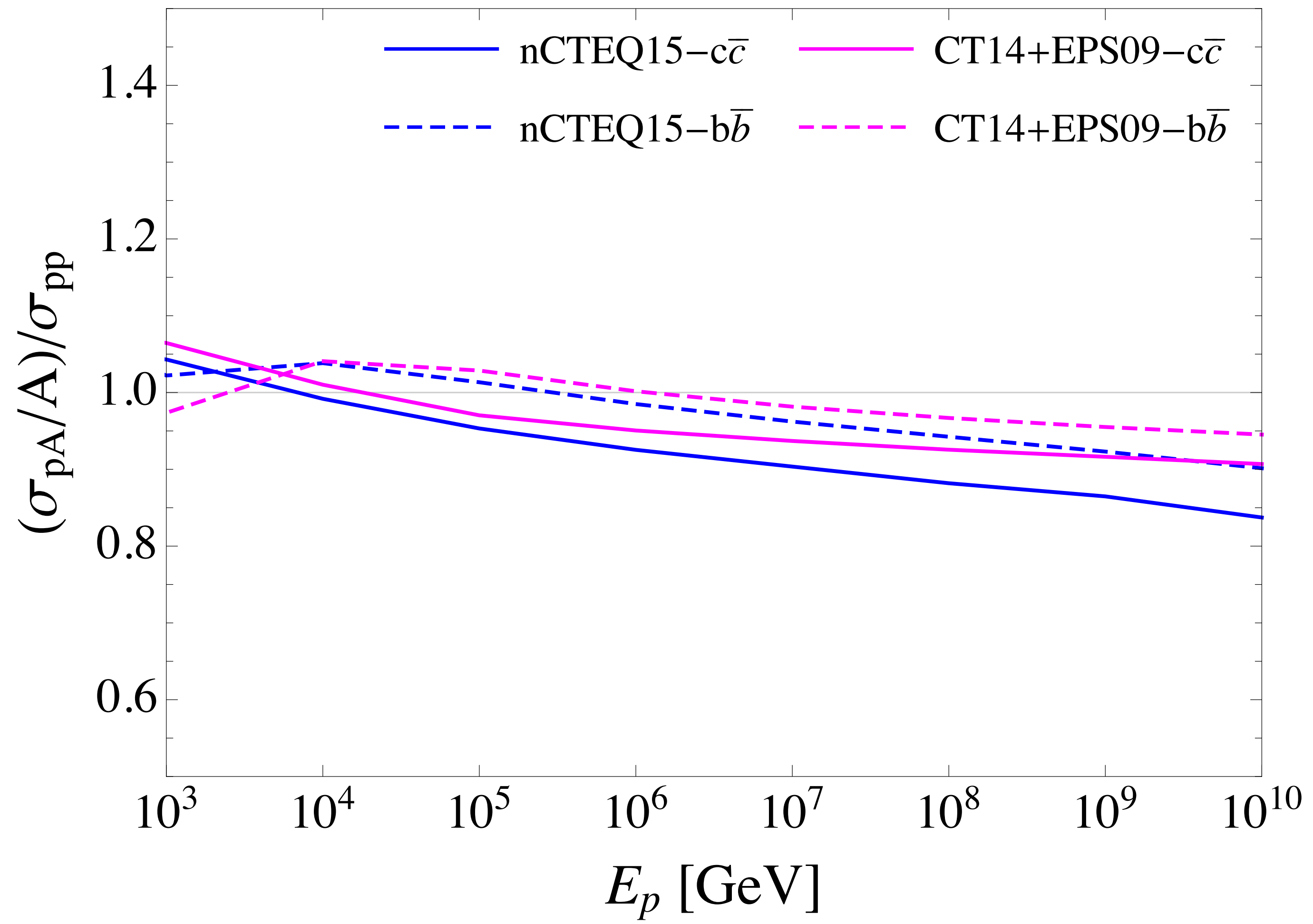

E_p	$\sigma(pp \to c\bar{c}X)$ [μb]		$\sigma(pA \to c\bar{c}X)/A$ [μb]		$[\sigma_{pA}/A]/[\sigma_{pp}]$	
	$M_{F,R} \propto m_T$	$M_{F,R} \propto m_c$	$M_{F,R} \propto m_T$	$M_{F,R} \propto m_c$	$M_{F,R} \propto m_T$	$M_{F,R} \propto m_c$
10^2	1.51	1.87	1.64	1.99	1.09	1.06
10^3	3.84×10^1	4.72×10^1	4.03×10^1	4.92×10^1	1.05	1.04
10^4	2.52×10^2	3.06×10^2	2.52×10^2	3.03×10^2	1.00	0.99
10^5	8.58×10^2	1.03×10^3	8.22×10^2	9.77×10^2	0.96	0.95
10^6	2.25×10^3	2.63×10^3	2.10×10^3	2.43×10^3	0.93	0.92
10^7	5.36×10^3	5.92×10^3	4.90×10^3	5.35×10^3	0.91	0.90
10^8	1.21×10^4	1.23×10^4	1.08×10^4	1.09×10^4	0.89	0.89
10^9	2.67×10^4	2.44×10^4	2.35×10^4	2.11×10^4	0.88	0.86
10^{10}	5.66×10^4	4.67×10^4	4.94×10^4	3.91×10^4	0.87	0.84

Differential charm cross section

Differential charm cross section in proton-nucleon collision as a function of the fraction of the incident beam energy carried by the charm quark.

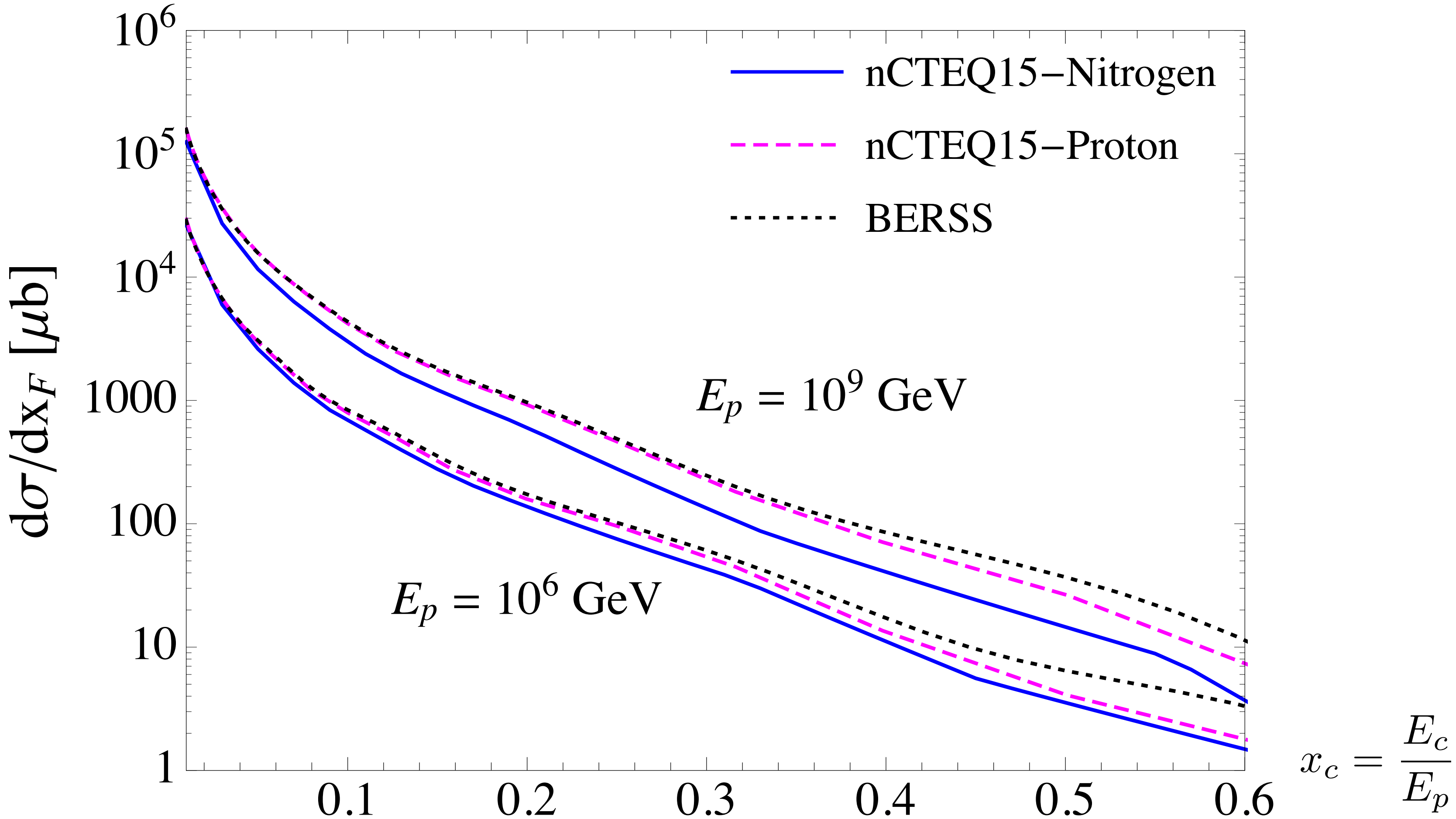

Differential charmed hadron cross section as a function of the energy: need to convolute with the fragmentation function

$$\frac{d\sigma}{dE_h} = \sum_k \int \frac{d\sigma}{dE_k}(AB \to kX) D_k^h\left(\frac{E_h}{E_k}\right)\frac{dE_k}{E_k} \qquad h = D^{\pm}, D^0(\bar{D}^0), D_s^{\pm}, \Lambda_c^{\pm}$$

Using Kniehl, Kramer fragmentation functions.

Comparison with LHCb data

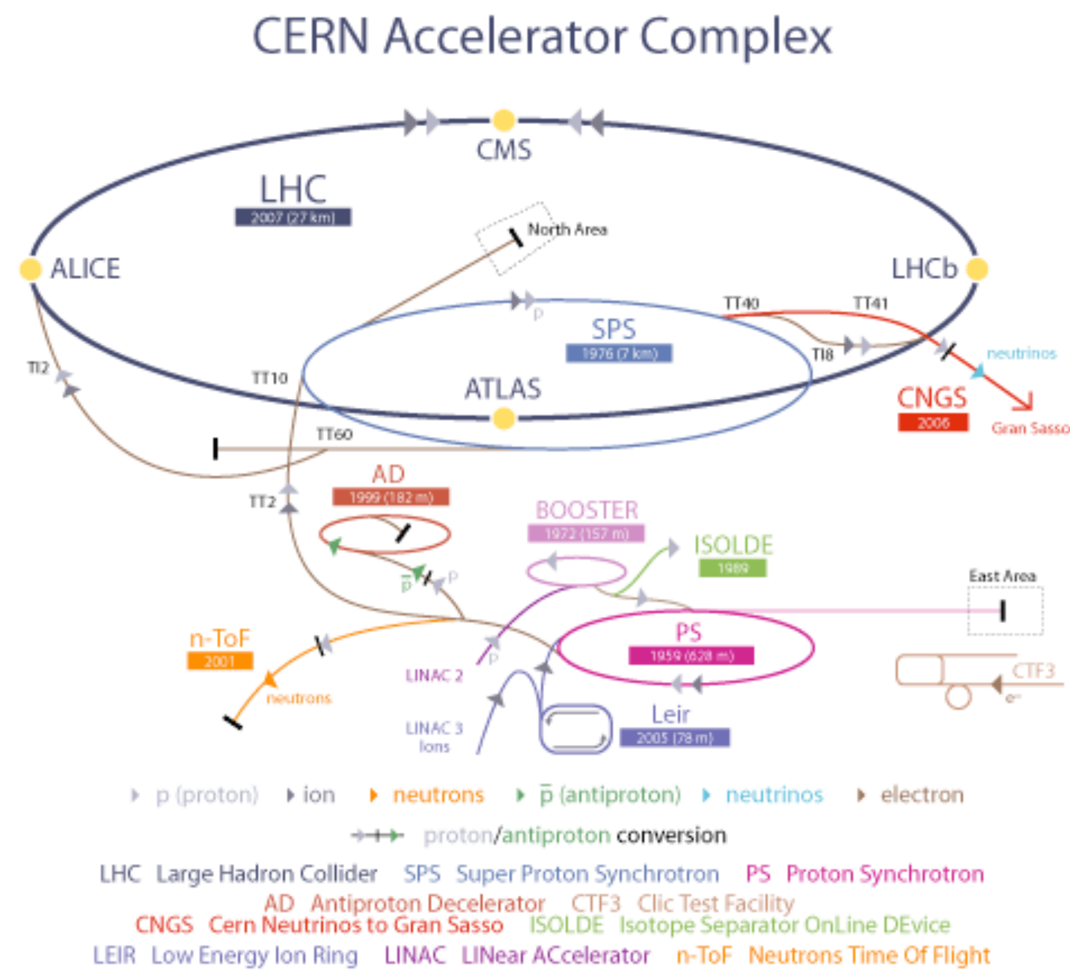

Specialized detector on the LHC ring.

Instrumentation in the forward region.

Sophisticated instrumentation to detect heavy particles.

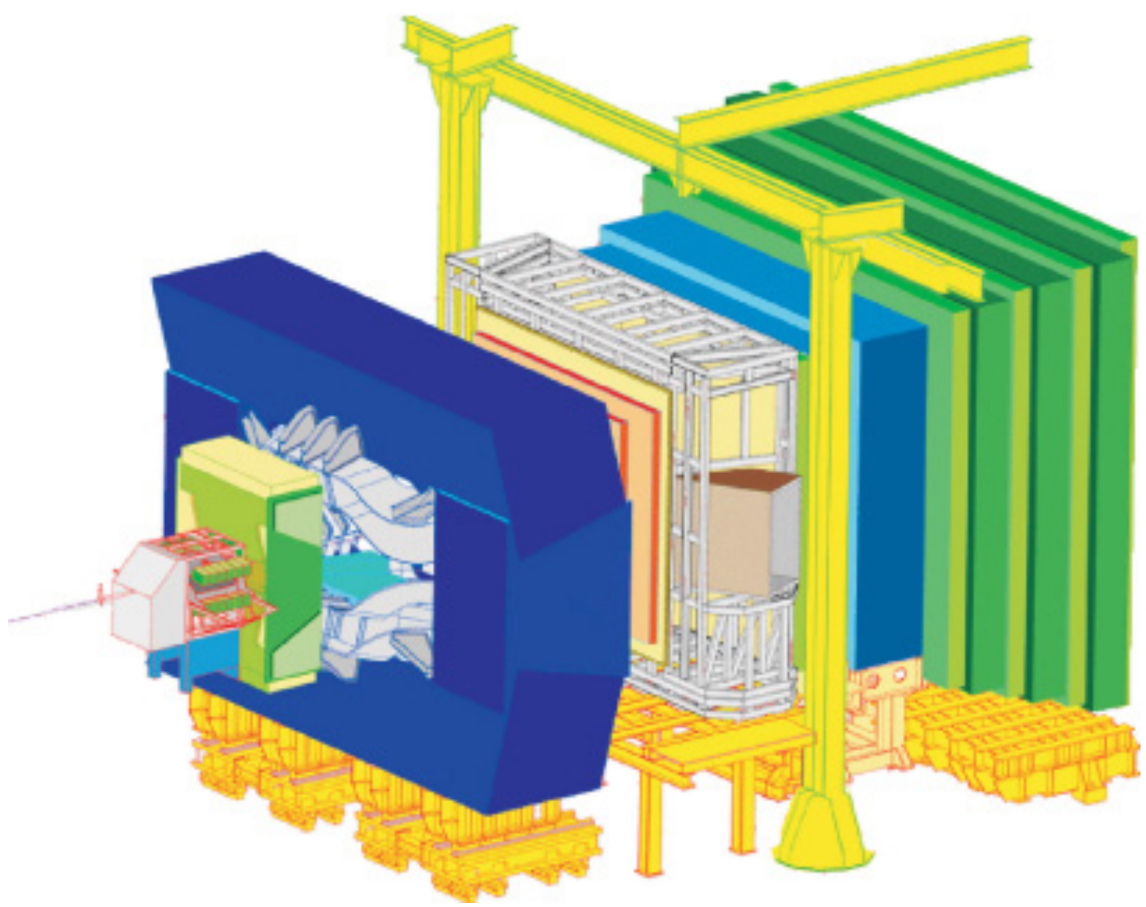

Compare with measurements on D mesons as a function of transverse momenta and rapidity.

Comparison with LHCb 7 and 13 TeV

Transverse momentum distributions at *forward rapidities*

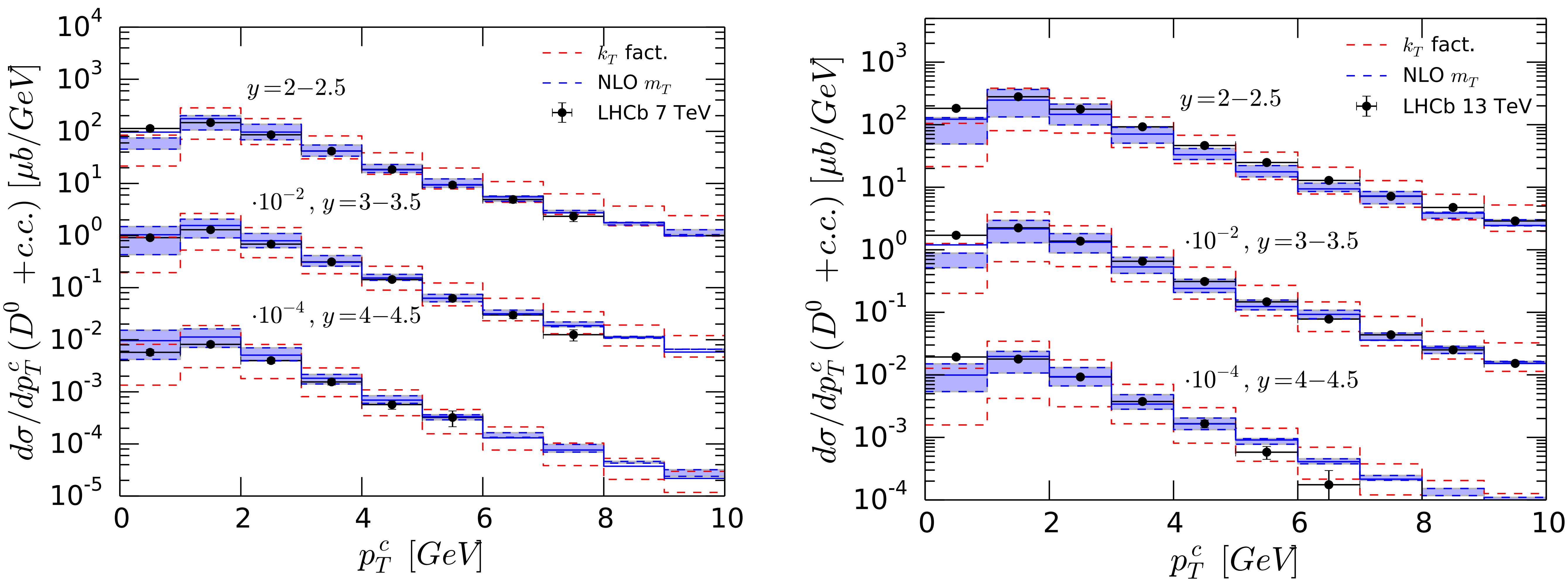

- NLO pQCD and k_T factorization consistent with each other.
- Bands on NLO pQCD calculation correspond to scale variation.
- Two lines in k_T factorization correspond to the saturation/no-saturation calculation.

Cosmic ray flux

Important ingredient for lepton fluxes: initial cosmic ray flux.

Parametrization by Gaisser (2012) with three populations and five nuclei groups: H,He,CNO,Fe,MgSi

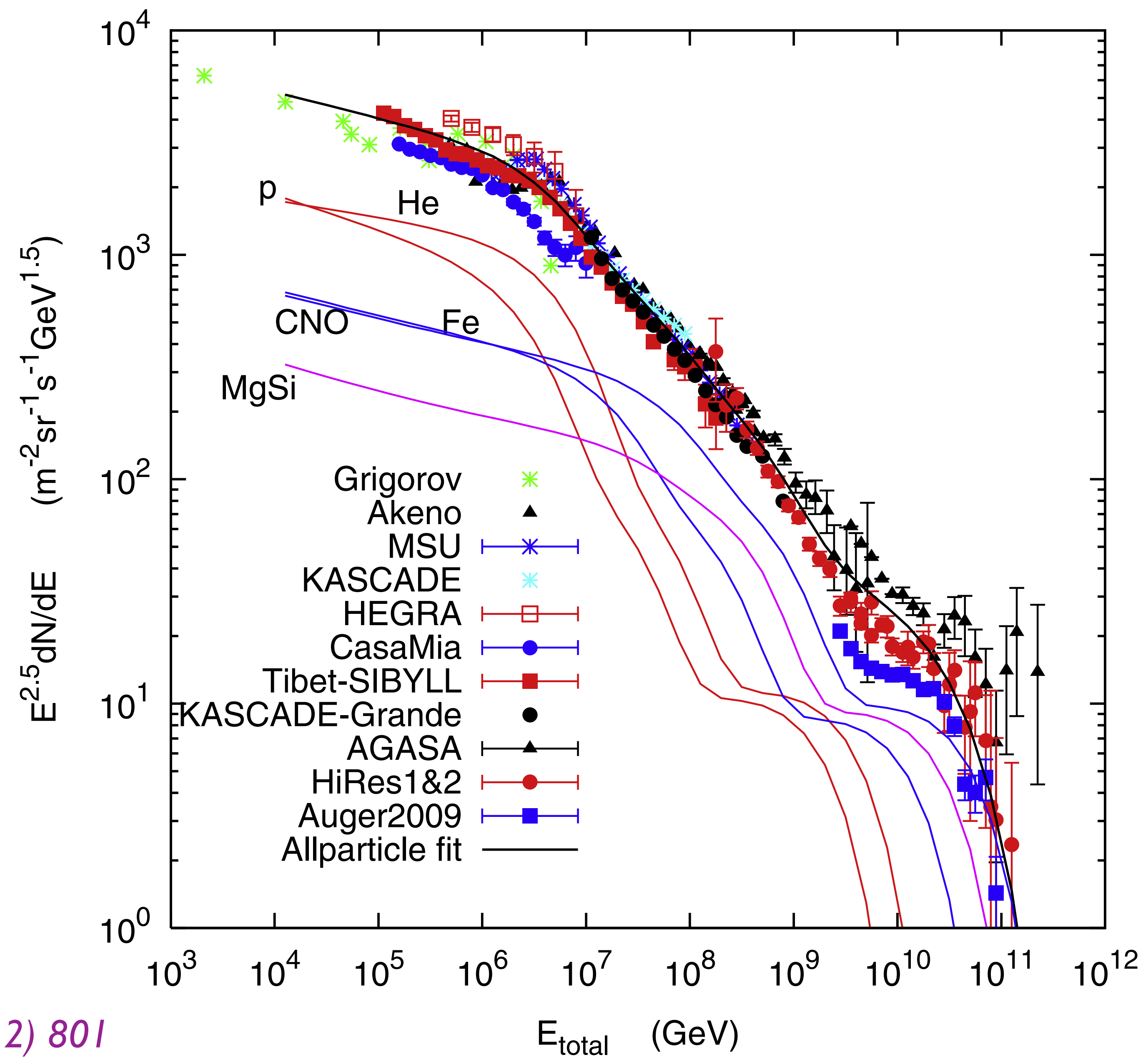

Gaisser,
Astroparticle Physics 35 (2012) 801

Cosmic ray flux

Multicomponent parametrization by Gaisser (2012) with three populations:

1st population: supernova remnants
2nd population: higher energy galactic component
3nd population: extragalactic component

$$\phi_i(E) = \sum_{j=1}^{3} a_{i,j} E^{-\gamma_{i,j}} \times \exp\left[-\frac{E}{Z_i R_{c,j}}\right]$$

$a_{i,j}$ normalization

$\gamma_{i,j}$ spectral index

$R_{c,j}$ magnetic rigidity

$E^c_{\rm tot} = Ze \times R_c$

$\phi = dN/d\ln E$

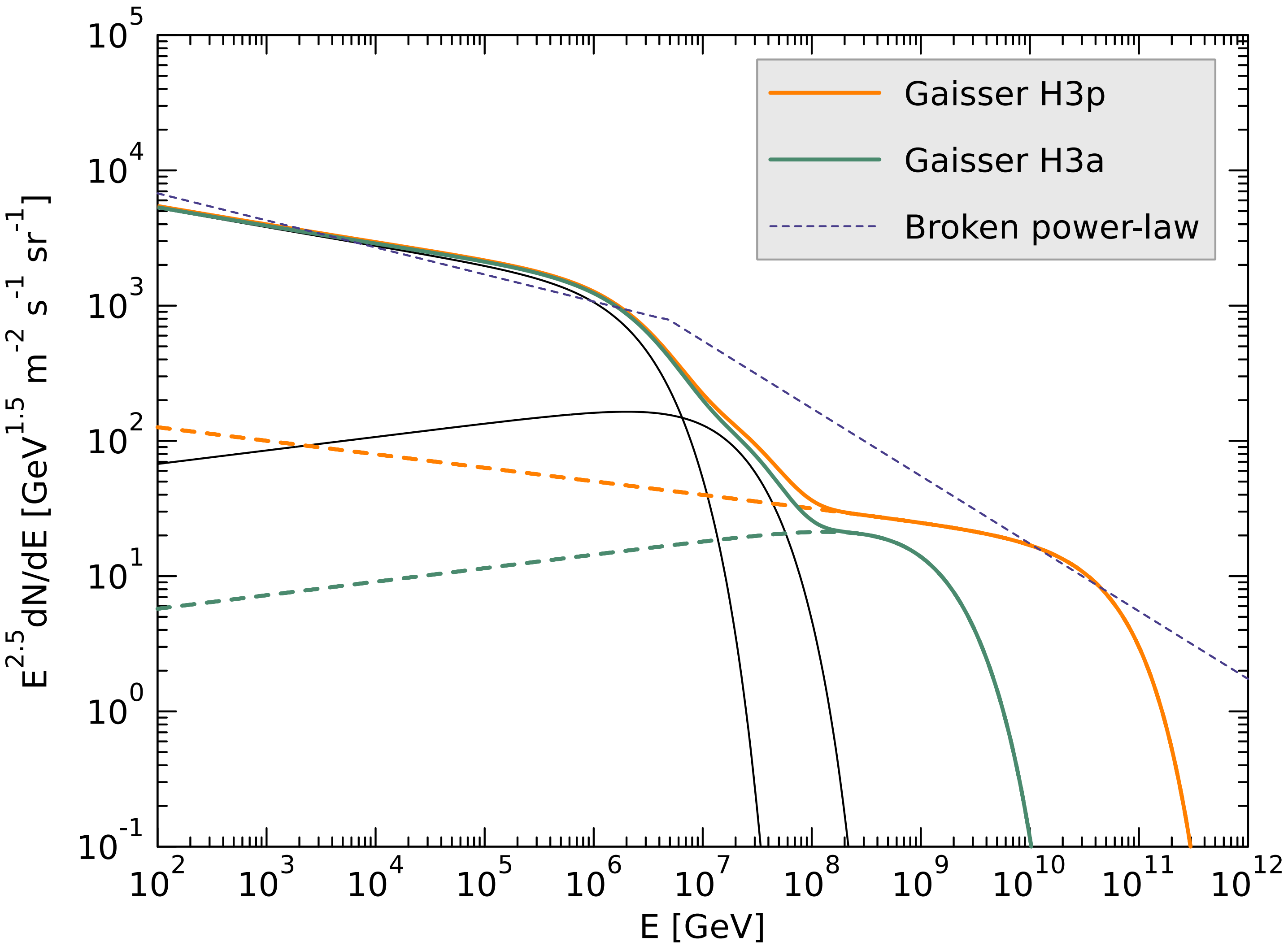

energy per nucleon

Converting to nucleon spectrum

$$\phi_{i,N}(E_N) = A \times \phi_i(AE_N)$$

for each component

This power law was used widely in previous evaluations of the prompt neutrino flux

$$\phi^0_p(E) = \begin{cases} 1.7\,E^{-2.7} & \text{for } E < 5\cdot 10^6 \text{ GeV} \\ 174\,E^{-3} & \text{for } E > 5\cdot 10^6 \text{ GeV,} \end{cases}$$

Development of air shower: cascade equations

Production of prompt neutrinos:

$$\text{p} \xrightarrow{\text{production}} \text{c} \xrightarrow{\text{fragmentation}} \text{M} \xrightarrow{\text{decay}} \nu$$

where M=$D^{\pm}, D^0, D_s, \Lambda_c$

Use set of cascade equations in depth X

$$X = \int_h^\infty \rho(h')dh'$$

$$\frac{d\Phi_j}{dX} = -\frac{\Phi_j}{\lambda_j} - \frac{\Phi_j}{\lambda_j^{dec}} + \sum_k \int_E^\infty dE_k \frac{\Phi_k(E_k, X)}{\lambda_k(E_k)} \frac{dn_{k\to j}(E; E_k)}{dE}$$

λ_j interaction length and $\lambda_j^{dec} = \gamma c \tau_j \rho(X)$ decay length

$\frac{dn_{k\to j}}{dE}$ production or decay distribution

$$\frac{1}{\sigma_k} \frac{d\sigma_{k\to j}(E, E_k)}{dE} \qquad \frac{1}{\Gamma_k} \frac{d\Gamma_{k\to j}(E, E_k)}{dE}$$

Need to solve these equations simultaneously assuming non-zero initial proton flux.

Neutrino fluxes

flux of $\nu_\mu + \bar{\nu}_\mu$

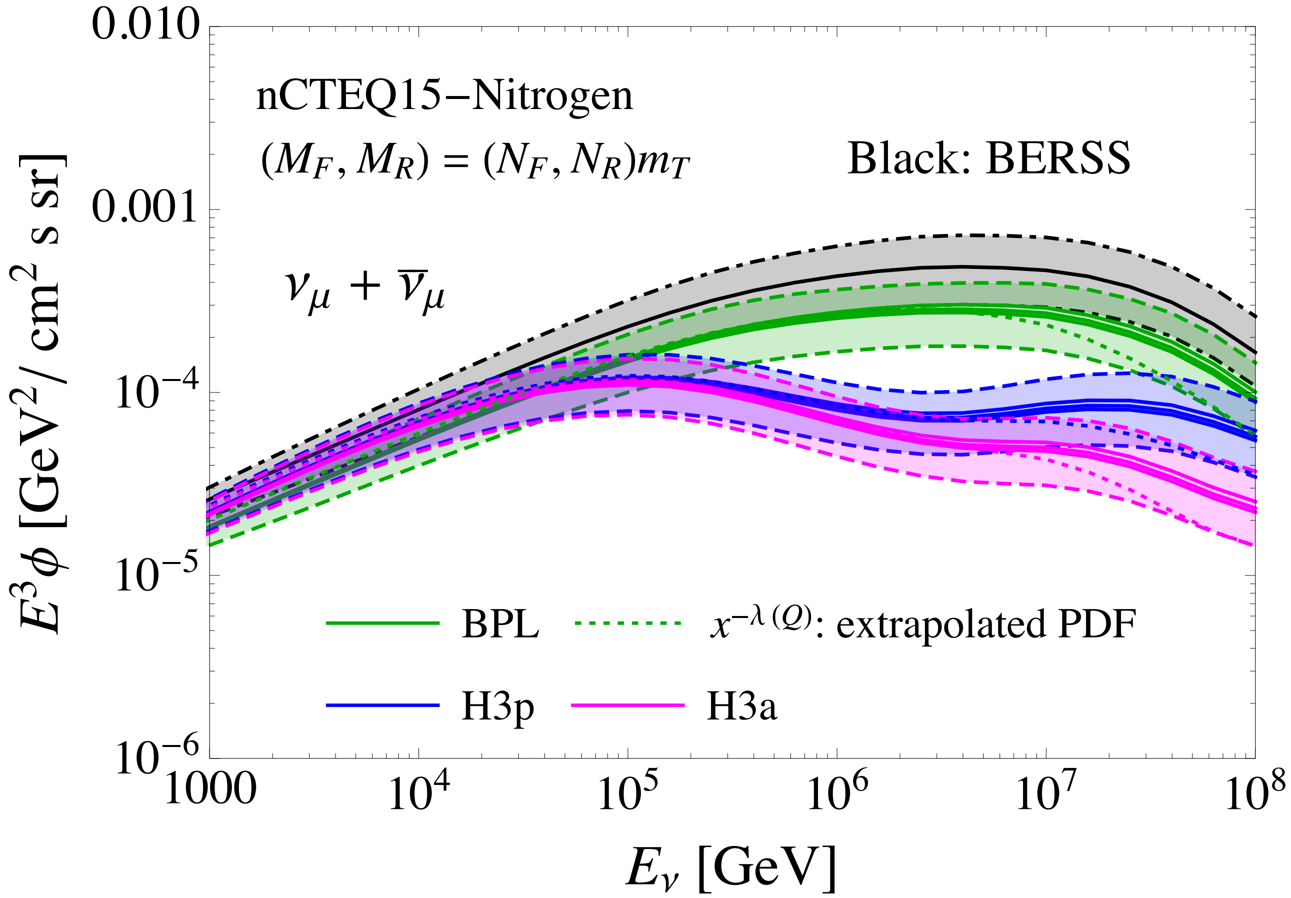

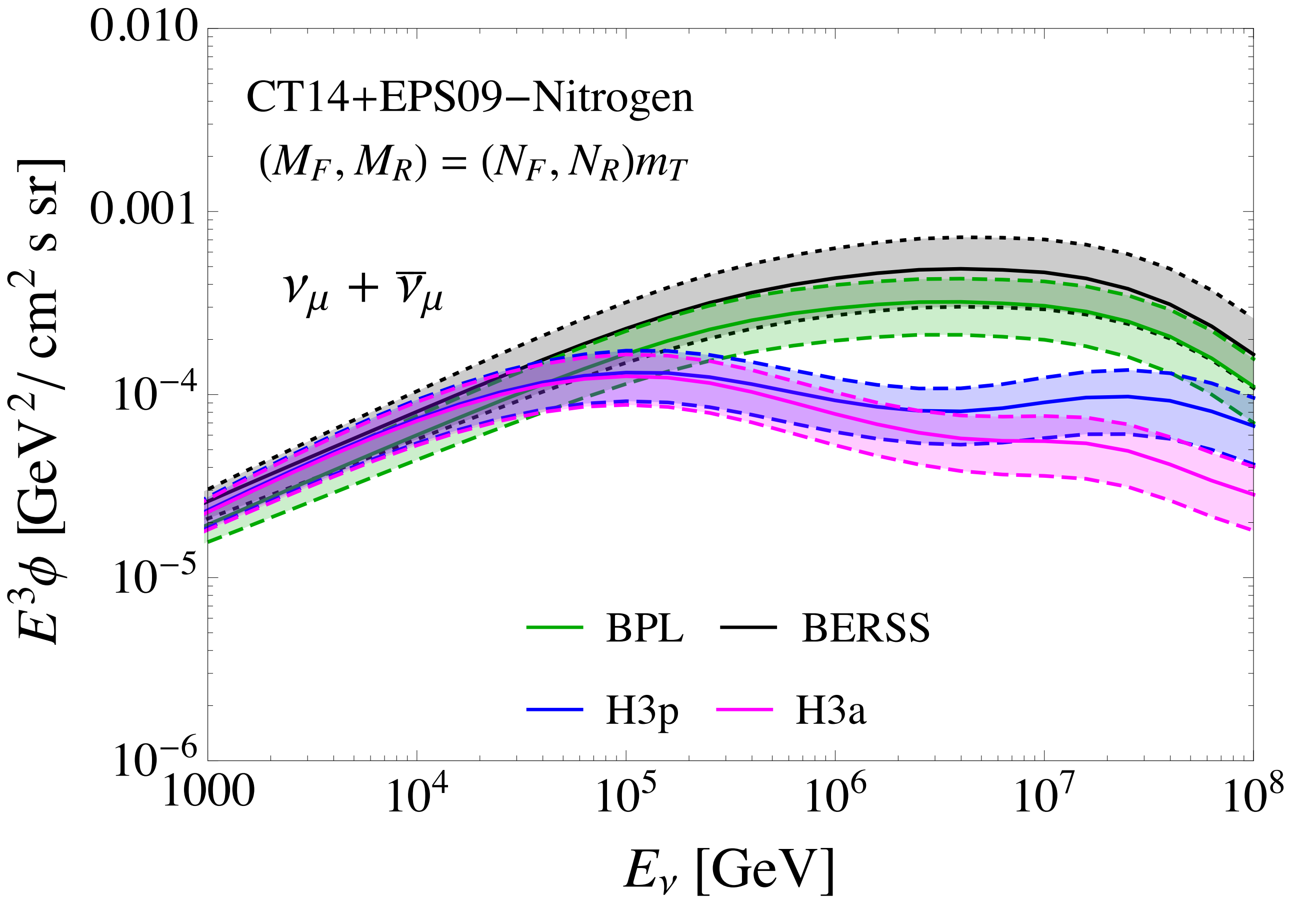

- Significant reduction (factor 2-3) due to the updated cosmic ray spectrum with respect to the broken power law.
- The reduction is in the region of interest, where prompt neutrino component should dominate over the atmospheric one.
- Black band: previous calculation.
- The updated fragmentation function reduces flux by 20%.
- B hadron contribution increases flux by about 5-10%.
- Nuclear effects: 20-35%.
- Combined effects: reduction by 45% at highest energies.

Predictions and IceCube limit

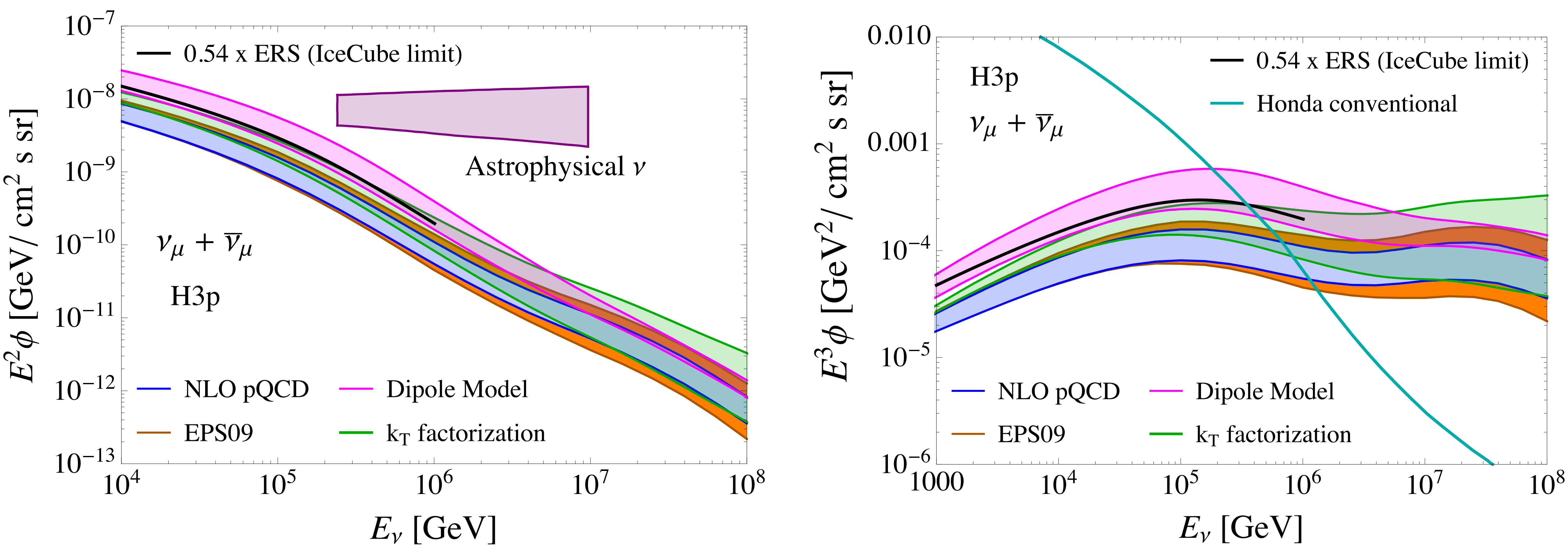

- Calculations consistent within the uncertainties .
- Overall the flux is well below the astrophysical flux measured by IceCube.

Prompt tau neutrino flux

From oscillations:

$\nu_\mu \to \nu_\tau$

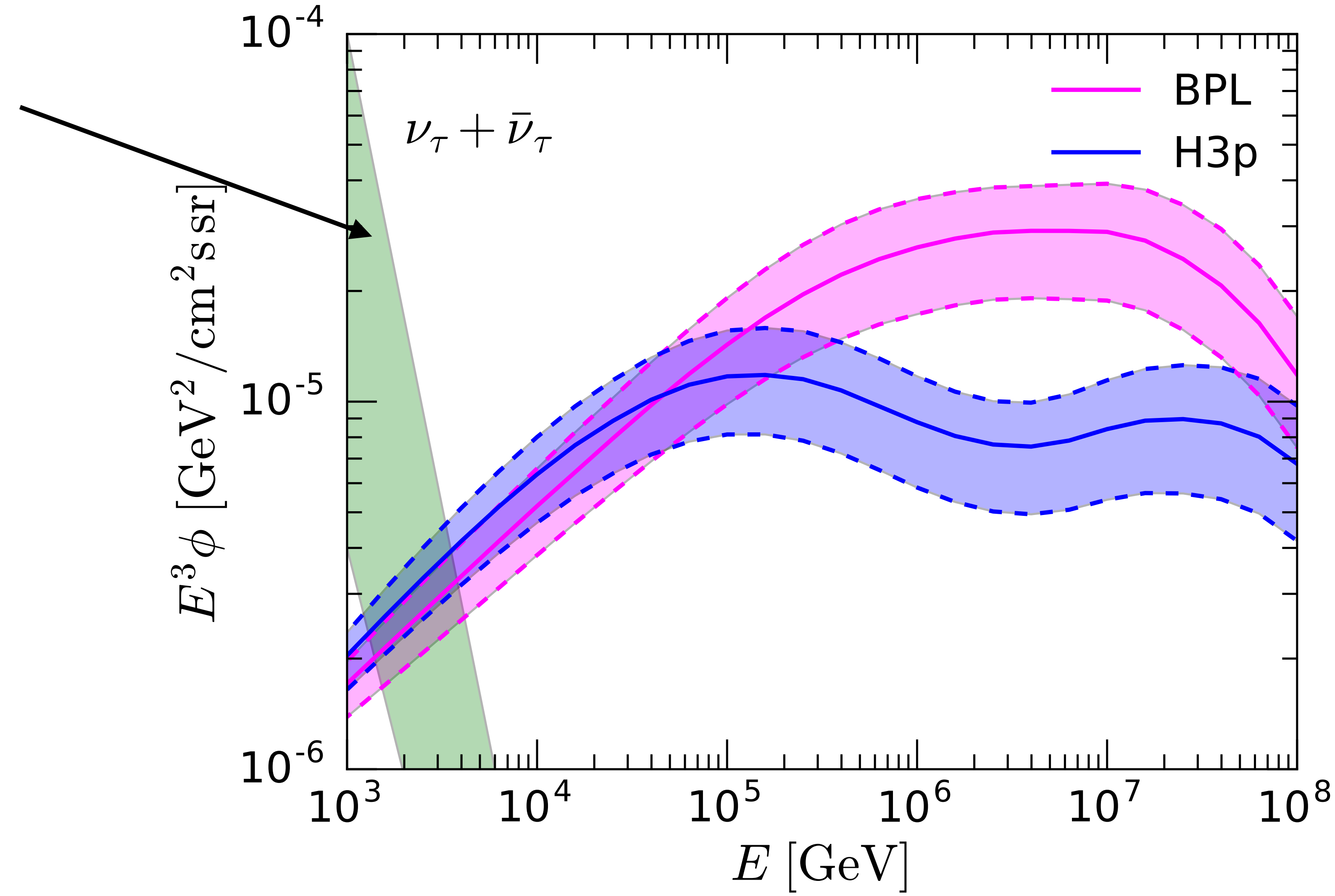

Tau neutrinos can be produced in the decays:

Direct $D_s \to \nu_\tau$

Chain $D_s \to \tau \to \nu_\tau$

Beauty $B^0, B^\pm$

Neutrinos from magnetars

Magnetar: neutron star with highest magnetic fields 10^{14}-10^{16} G

Sources of X and gamma rays

Could also be the sources of highly energetic protons and therefore also neutrinos (from pp and pγ)

Image credit: ESO/L. Calçada)

Neutrino fluence from a nearby magnetar

Prompt neutrinos can be dominant

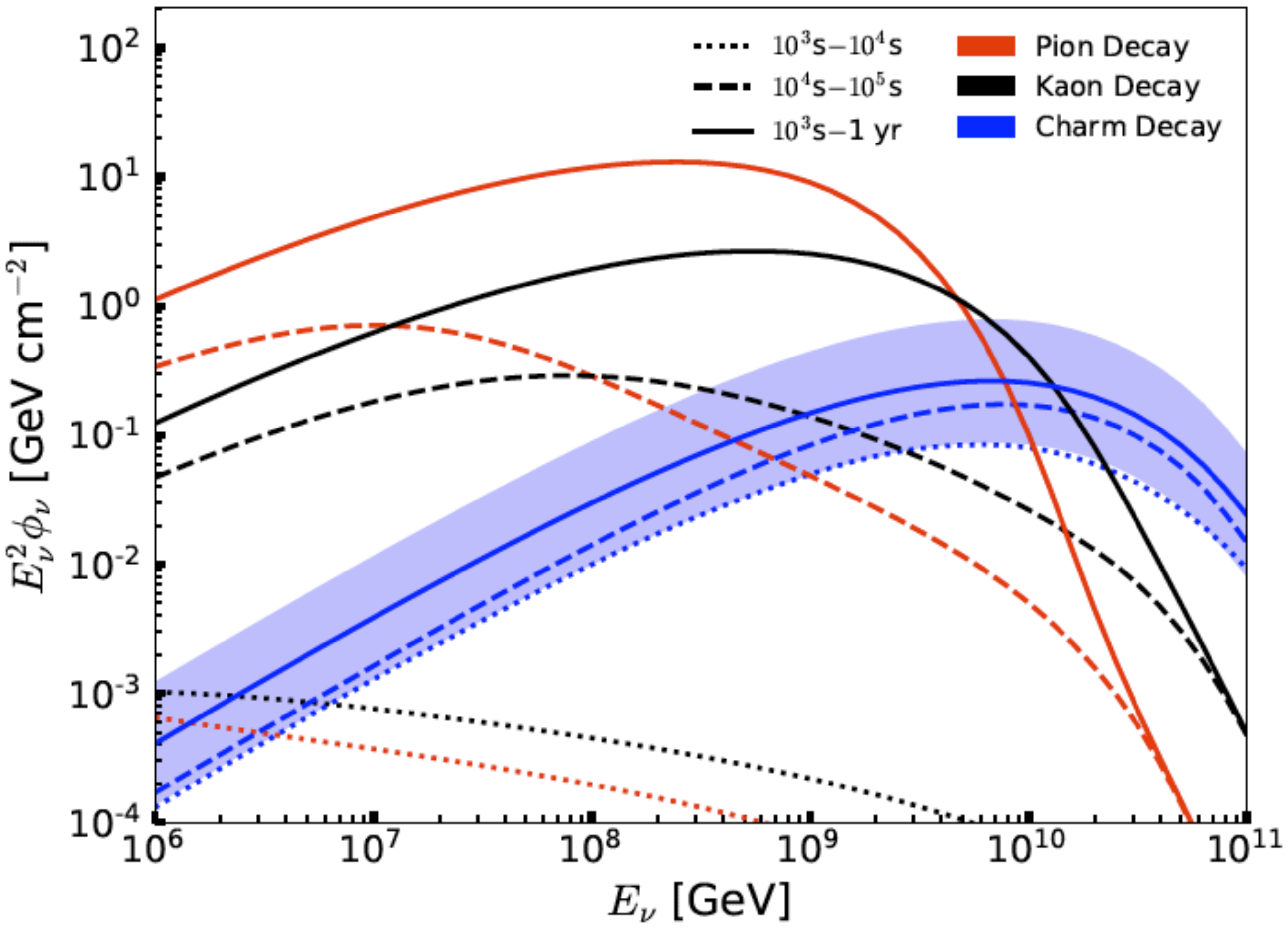

Summary and outlook

- Highly energetic neutrinos interact with cross section in the range dominated by small x phenomena
- Nuclear effects rather small, but large uncertainties in this region. CGC type effects could lead to larger suppression
- Prompt neutrino production from charm sensitive to details of small x dynamics.
- Nuclear effects in the target. Reduction of the flux by about 20-35%. Estimate of nuclear corrections within the NLO pQCD consistent with the small x calculation.
- Other calculations also on the market: consistent but still large uncertainties. Largest uncertainties due to the QCD scale variation, PDF uncertainties and CR flux.
- Predictions for neutrinos from magnetars. Charm component may be dominant for some parameter space.
- Outstanding questions: CR initial flux(composition); fragmentation (forward production, hadronic-nuclear environment, differences between PYTHIA and fragmentation functions).